THE JOURNAL OF PHYSICAL CHEMISTRY A

Article

pubs.acs.org/JPCA

# 11,11-Dimethyl-1,6-methano[10]annulene—An Annulene with an Ultralong CC Bond or a Fluxional Molecule?

Alan Humason, Wenli Zou, and Dieter Cremer*

Computational and Theoretical Chemistry Group (CATCO), Department of Chemistry, Southern Methodist University, 3215 Daniel Avenue, Dallas, Texas 75275-0314, United States

Supporting Information

**ABSTRACT:** Extensive quantum chemical calculations involving more than 20 different methods and including vibrational, temperature, entropic, and environmental corrections suggest that 11,11-dimethyl-1,6-methano[10]annulene (**1**) is characterized by a broad, asymmetric single well potential minimum in which the molecule can carry out a large-amplitude vibration. This result is obtained by using CASPT2(14,14) and CCSD(T) together with a VTZ basis set. The average $R$(C1C6) distance of **1** is close to 1.8 Å, in agreement with X-ray diffraction measurements. Lower level methods fail because a reliable account of the electronic structure of bridged annulenes requires a balanced description of nondynamical and dynamical electron correlation effects as well as a correct assessment of bridge−annulene interactions. An independent determination of the distance $R$ using the mean deviation between the calculated and measured $^{13}C$ NMR chemical shifts of **1** leads to a value of 1.79 Å. By using electron density, energy density, and the local C1C6 stretching mode, it is demonstrated that the covalent bond ceases to exist at 1.695 Å and that for larger $R$ values through-space homoaromatic interactions lead to some stabilization. The peculiar potential of **1** is shown to be a result of the interaction of the methyl groups with the perimeter CC bonds bisected by the symmetry plane of the molecule. CASPT2(14,14), CASPT2(10,10), CCSD(T), and BD(T) calculations were also used to provide for the first time reliable descriptions of the valence tautomeric potentials for the parent molecule, 1,6-methano[10]annulene (**2**), and the system 1,3,5-cycloheptatriene−norcardiene (**3**). In the latter case, calculations confirm a previous kinetic measurement of the free activation energy but correct NMR-based estimates. The methodology described can be applied to other annulenes and fullerenes.

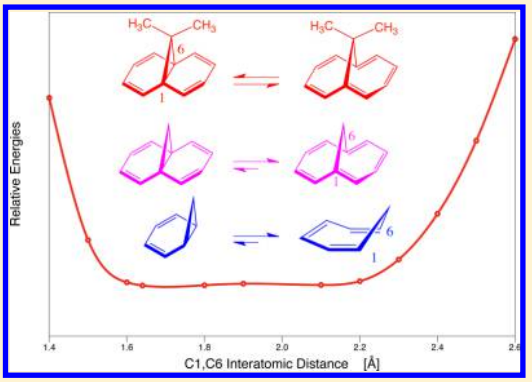


## 1. INTRODUCTION

For the purpose of getting a better understanding of the nature of the chemical bond, chemists have always been interested in answers to questions such as "What is the strongest (weakest) or shortest (longest) bond ever observed or may be in general possible?"[1−3] Since the chemical bond is a concept rather than an observable quantity, which can be extensively described by suitable measurements, answers to these questions may have only heuristic value if not handled within a well-defined model of the chemical bond. The typical superlative questions lead only to useful answers if they are defined as precisely as possible, thus clarifying definitions and evaluation methods within given models and concepts.

In this work, we focus on (through-space or through-bond) interactions between two C atoms, which are separated by 1.8 Å and investigate the question whether these interactions lead to a covalent bond. This implies that we contrast the interaction in question on the background of other long CC bonds, clarify which bonding models and definitions we will use, and why the investigation is important in connection with a molecular system that has puzzled chemist for almost 50 years (see below).

Typical electron pair bonds between neighboring C atoms can be lengthened as a consequence of (i) exchange (steric) repulsion between bulky substituents,[3−8] (ii) a loss of bonding electrons or electron density leading to electron deficient bonding,[9−13] (iii) the occupation of antibonding orbitals, or (iv) decoupling of spin pairs leading to open singlet states (e.g., *pancake bonds*).[6,14−16] (v) In turn, interacting CC atoms at large distances can be clamped together by electrostatic attraction when highly polar or ionic,[17−21] by dispersion interactions,[3] or by connecting bridges enforcing a "cage"-topology (*clamped bonds*[22]). Packing effects in a solvent cage or in a crystal could also be possible. Often these effects cannot be clearly separated because they support each other. Many examples have been given for such long CC bonds or CC interactions where one has to ask in each case whether a stable molecule or a labile intermediate was obtained.

**Special Issue:** 25th Austin Symposium on Molecular Structure and Dynamics

**Received:** August 16, 2014
**Revised:** October 20, 2014
**Published:** October 21, 2014

The existence of a chemical bond can be verified using experimental data. Pauling suggested that *a chemical bond is given when two atoms or fragments are kept together by some forces that it seems to be justified to consider the resulting entity as an independent molecule.*[1] Less vague definitions of a chemical bond can be obtained utilizing energy, geometrical, orbital or density characteristics. There is a myriad of bond definitions within specific models. We will avoid an explicit discussion of these definitions and models by exclusively focusing in this work on measurable quantities such as electron density distribution, vibrational frequencies, NMR chemical shifts, and indirect spin−spin coupling constants (SSCCs). From these properties we will determine quantities that make it possible to characterize the CC interactions investigated in this work as being covalent bonding or just through-space interactions.

The target system **1** investigated in this work (see Figure 1) belongs to the group of bridged [10]annulenes, the parent

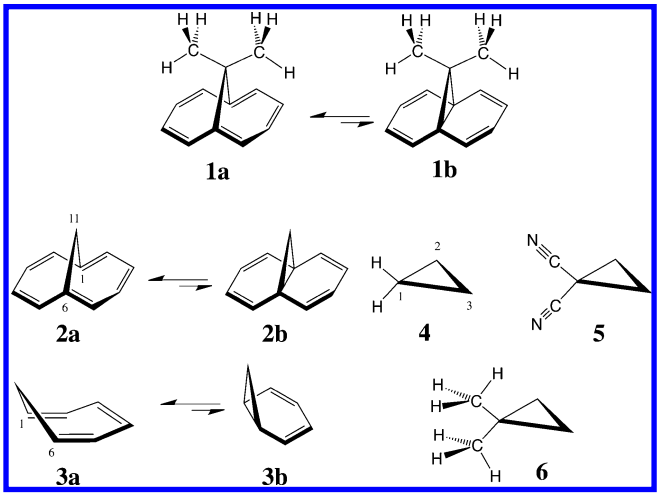


**Figure 1.** Molecules investigated in this work.

member of which, 1,6-methano[10]annulene (**2**), was first synthesized by Roth and Vogel in 1964.[23] Annulene **2** was experimentally characterized as an aromatic 10$\pi$-system fulfilling the Hückel $4n + 2$ rule, however with a distorted ring perimeter and a C1C6 distance $R$ of 2.235 Å;[24,25] that is, it adopts structure **2a** rather than that of the bisnorcaradiene (tricyclo[4.4.1.0$^{1,6}$]undeca-2,4,7,9-tetraene) form **2b** (see Figure 1), as was verified in dozens of experimental investigations[23−37] as well as computational investigations.[32,38−43] Therefore, it was an unexpected result when in the early 1970ies the 11,11-dimethyl derivative **1**, also synthesized by the Vogel group, was found to adopt according to X-ray diffraction studies[44] a "tricyclic" structure with an $R$ value close to 1.8 Å (1.827 and 1.771 due to 2 molecules in the unit cell[44]) that speaks in favor of structure **1b** rather than **1a**. With the discovery that the corresponding 11-cyano-11-methyl derivative had similar $R$ values[45] and the dicyano derivative had even an $R$ value of 1.558 Å,[44,46] the existence of a bisnorcaradiene form was fully confirmed.

Günther and others carried out NMR (nuclear magnetic resonance) investigations on valence tautomeric systems such as **1** and **2** and showed that any shift to the bisnorcaradiene or annulene form leads to characteristic changes in the $^{13}C$ chemical shifts.[47,48] These studies were latter confirmed by Frydman and co-workers[49] as well as Dorn and co-workers,[50] who all documented a strong temperature dependence of the $^{13}C$ NMR signals of **1**. Hence, the basic question was whether bridged annulenes could be considered as fluxional systems which changed their bonding structure according to the valence tautomeric rearrangement indicated in Figure 1 or whether they possessed long CC bonds.

Since the available experimental evidence for **1** favored the bisnocaradiene form, the molecule was considered as the neutral hydrocarbon with the longest (covalent) cyclopropane C(sp$^2$)C(sp$^2$) bond. Therefore, **1** was computationally investigated multiple times to rationalize the bonding situation.[32,39−43] However, this work was hampered by the fact that the size of the molecule and the requirements for the basis set made state-of-the-art computations that guarantee high accuracy results extremely difficult. In this work, we will close this gap in the description of **1** by carrying out coupled cluster and multireference calculations and providing a reliable description of the electronic structure. The following questions will be answered in this work: (i) What is the exact shape of the C1C6 potential of **1** (single or double well)? (ii) Which electronic factors determine the shape of the potential? For example, are there specific interactions between bridge and $\pi$-perimeter, which may influence the structure and dynamics of **1**? (iii) How does $\pi$-delocalization in **1** and **2** compare with that of benzene? (iv) What level of theory is required to guarantee a reliable description of the properties of **1** (or **2**)? (v) Do temperature, entropy, or environmental effects such as solvation or crystal packing influence the shape of the potential? (vi) How does the valence tautomeric behavior of **1** relate to that of other closely related molecules such as **2** or the system cycloheptatriene-norcaradiene (**3**, Figure 1)? (vii) Are there other observations which may lead to a confirmation of the shape of the potential of **1**? (viii) Does **1** contain a long covalent C1C6 bond, as is generally believed today, and if so, is this the longest C(sp$^2$)C(sp$^2$) single bond of an uncharged hydrocarbon ever observed?

We will present the results obtained in this work in the following way. In section 2, the computational means used in this work are described. The results and discussion are presented in section 3. The chemical relevance of this work is outlined in section 4. Conclusions are drawn in section 5.

## 2. COMPUTATIONAL METHODS

The C1C6 potential energy curves (PECs) of molecules **1**, **2**, and **3** were calculated by stepwise increasing of the distance $R$ = $R$(C1,C6) from 1.4 to 2.6 Å in increments of 0.1 Å, and then optimizing all other geometrical parameters of the molecule in question. The energy values thus obtained were fitted to a suitable analytic function using standard fitting techniques. For the analytical PECs thus obtained, the $R$ value(s) of the minimum or minima were determined and then used for an accurate reoptimization. This procedure was carried out at the Hartree−Fock (HF) level, density functional theory (DFT) level using various LDA, GGA, hybrid, and double-hybrid functionals (see below) as well as the second order Møller−Plesset Perturbation Theory (MP2) level of theory.[51,52]

Using the geometries determined in the first step, single point calculations with a variety of electron correlation WFT (wave function theory) methods were carried out to obtain more accurate PECs. It turned out that the use of different geometries based on HF, DFT, or MP2 calculations did not change the resulting PECs significantly. The vibrational frequencies obtained with DFT methods such as B3LYP[53,54] or $\omega$B97X-D for **2a** agree better with measured values[34] than


dx.doi.org/10.1021/jp5082966 | J. Phys. Chem. A 2015, 119, 1666−1682

HF or MP2 frequencies, thus indicating that thermochemical corrections calculated with DFT are preferable. Therefore, we present in this work for reasons of consistency only the PECs based on geometries obtained with the two XC functionals ωB97X-D and B3LYP.

For the purpose of studying the influence of dynamical electron correlation on the shape of the PEC, we used *n*th order MP (MP*n*) theory and Coupled Cluster theory with HF or alternatively Brueckner (B) orbitals. Correlation effects were determined by considering all S (single), D (double), and T (triple) or perturbative T (denoted as (T)) and Q (quadruple) excitations. In all, we used MP2, MP3, MP4(SDQ), MP4-(SDTQ),[51,52] CCSD,[55] BD,[56] CCSD(T),[57] and BD(T).[58]

The influence of nondynamical electron correlation effects was studied utilizing CASSCF (complete active space self-consistent field),[59] CASPT2 (CASSCF with second order MP perturbation theory),[60] and NEVPT2 (*n*-electron valence perturbation theory of second order).[61] For these multi-reference calculations, active spaces of **1a** and **2a** with 10 electrons (all π) and 10 orbitals (5 occupied π-orbitals and the lowest 5 virtual π-MOs) were selected. In the case of **3a** the corresponding (6,6)-active space was chosen. In the valence-tautomeric rearrangement of the annulene (triene) form to the bisnorcaradiene (norcaradiene) form, π-orbitals are converted into C1C6 σ and σ* orbitals and other σ-orbitals mix with the π-orbitals, changing their character. Apart from this, one has to consider that π- and σ-orbitals can change their energies and order. Therefore, it was carefully monitored that when changing *R* the (10,10) or (6,6) active spaces were consistently maintained along the path defined by *R*.

This procedure led to unsolvable problems in the case of system **3** where the nonplanarity of **3** (see Figure 1) leads to strong σ−π mixing. We found that a consistent description can only be obtained by a (10,10) active space for the norcaradiene form, which includes besides the π-system also the 6 electrons and 6 Walsh orbitals (for pictorial representations of these orbitals, see ref 62.) of the cyclopropyl ring. By converting one of the Walsh orbitals into a π-orbital for increasing *R*, a consistent (10,10) description could be found for system **3a**. The following orbitals comprised the (10,10) space of **3b**: 10a′, 14a′, 19a′, 8a″, 12a″, 16a″ (Walsh orbital set), 15a′, 16a′, 10a″, 11a″ (π-orbital set).

This observation encouraged us to improve the multi-reference description of systems **1** and **2** in a similar way, repeating the PEC calculations with a (14,14) active space including the Walsh orbitals of the cyclopropyl rings of the bisnorcaradiene forms and the σ (σ*) orbitals of the C1C11 and C6C11 bonds of the annulene. For **1b**, the following orbitals established the (14,14) space: $14a_1$, $16a_1$, $9b_1$, $12b_1$, $17b_1$, $15b_2$ (Walsh orbital set); $15a_1$, $17a_1$, $10b_1$, $11b_1$, $12b_2$, $13b_2$, $8a_2$, $10a_2$ (π-orbital set). In the case of **2b**, the (14,14) space comprised the following: $10a_1$, $13a_1$, $17a_1$, $8b_2$, $11b_2$, $14b_2$ (Walsh orbital set); $12a_1$, $15a_1$, $9b_1$, $10b_1$, $9b_2$, $10b_2$, $7a_2$, $9a_2$ (π-orbital set).

Clearly, a (34,34) active space would have been ideal for the inclusion of all σ−π interactions. However, this approach was outside the computational possibilities. We also used the smaller active space for multireference averaged quadratic coupled cluster theory (MR-AQCC).[63] In addition, systems **1a**/**1b** and **2a**/**2b** were also investigated utilizing the DIP-EOM-CCSD (equation of motion double ionization potential coupled cluster with S and D excitations) method.[64]

For the HF, DFT, and MP2 PECs, the corresponding enthalpy and free energy curves were determined by calculating vibrational, thermal, and entropy corrections. In this way, the enthalpy and free energy curves associated with the PEC could be analyzed. At the DFT level, solvation effects were tested with the PCM (polarizable continuum model) of Tomasi and co-workers[65] where the dielectric constant ϵ was increased from 2 to the value of methanol (ϵ = 32.7[66]), which was used as a solvent for some of the NMR investigations of **1**.[49,50]

The influence of the methyl groups on the stability of the annulene was determined by utilizing isodesmic reaction energies. For reasons of comparison, cyclopropane (**4**), 1,1-dicyanocyclopropane (**5**), and 1,1-dimethylcyclopropane (**6**) were investigated. All these calculations were carried out at the B3LYP and ωB97X-D levels of theory. Throughout this work Pople's augmented VTZ basis 6-311G(d,p)[67] was employed at all levels of theory. We also tested the necessity of using diffuse functions by applying Dunning's aug-cc-pVTZ basis set. In the case of B2PLYP-D, the inclusion of diffuse functions only led to small changes in the relative energies of **1**. Because of computational limitations in the case of the WFT methods, we employed the smaller VTZ basis throughout this work.

Several molecular properties and their changes along the PEC were also calculated and analyzed. These included the NBO (natural bond order) charges,[68] the charge transfer between bridge and π-perimeter in the cases of **1** and **2**, electron densities, energy densities, NMR (nuclear magnetic resonance) properties, and local vibrational mode properties. The last three properties will be shortly discussed in the following.

**Electron density analysis.** The electron density distribution $\rho(\mathbf{r})$ was analyzed with the help of topological analysis[69] to determine all CC and CH bond critical points $\mathbf{r}_b(CC)$ and $\mathbf{r}_b(CH)$ as well as the ring critical points $\mathbf{r}_r$ of $\rho(\mathbf{r})$. In this connection, the Cremer−Kraka definition of covalent bonding was used: (i) A zero-flux surface and bond critical point $\mathbf{r}_b$ has to exist between the atoms in question (necessary condition). (ii) The local energy density $H(\mathbf{r}_b)$ must be negative and thereby stabilizing (sufficient condition for covalent bonding). A positive $H(\mathbf{r}_b)$ indicates a dominance of electrostatic interactions.[70,71] The Cremer−Kraka criterion reveals at which *R* value the C1C6 bond ceases to exist (or is formed).

**NMR analysis.** $^{13}C$ and $^{1}H$ magnetic shieldings and chemical shifts (using tetramethylsilane as reference) were calculated for all systems using the gauge-invariant atomic orbital (GIAO) method[72] in connection with B3LYP, which leads to useful $^{13}C$ values.[73] For the determination of $R(\mathbf{1})$ in solution, the *NMR-ab intio* method of Cremer and co-workers[74,75] was used. Since the $^{13}C$-NMR chemical shifts of **1** are known,[50] the deviation between measured and calculated $^{13}C$ chemical shifts along the PEC was calculated and the minimum of their mean (absolute) deviation was determined, because the latter is a reliable indicator of the *R* value of **1** in solution. In addition, all $J(^{13}C^{13}C)$, $J(^{1}H^{1}H)$, and $J(^{13}C^{1}H)$ indirect spin−spin coupling constants (SSCCs) of **1** were calculated using the method of Cremer and co-workers.[76] Those SSCCs which show the strongest dependence on the valence-tautomeric rearrangement were analyzed as functions of *R*.

**Local vibrational mode analysis.** Generalized local vibrational modes are the unique equivalents of the $3N - L$ (*N*: number of atoms; *L*: number of translations and rotations) generalized normal vibrational modes and their properties


dx.doi.org/10.1021/jp5082966 | J. Phys. Chem. A 2015, 119, 1666−1682

(local mode frequency $\omega_a$, mass $m_a$, force constant $k_a$, intensity $I_a$) were calculated according to the theory of Konkoli and Cremer[77−79] and its extension by Zou and Cremer.[80−82] The local CC stretching force constant $k_a$ is a reliable measure of the strength of the corresponding bond and can be used to calculate with the help of a power relationship the bond strength order (BSO) $n$:[2,83−85] $n(CC) = a(k_a)^b$. Parameters $a$ and $b$ were determined in this work to be $a = 0.3116$ and $b = 0.8066$, utilizing ethane and ethene as suitable references with $n(CC) = 1$ and 2, respectively. Additionally, $n(CC) = 0$ was imposed for $k_a = 0$. The calculated BSOs provide a measure for the degree of $\pi$-delocalization in aromatic molecules, as was recently shown by Kalescky and co-workers.[86] These authors derived an AI (aromaticity index) based on benzene (AI = 1.0) and "Kekule benzene" (1,3,5-cyclohexatriene: AI = 0) where in the latter case 1,3-butadiene was used to define a suitable reference geometry. A fully aromatic system is predicted to have all conjugated CC bonds equal to the benzene CC bond length, whereas deviations from this value indicate the degree of bond alternation and bond strengthening (weakening).[86] AI values were calculated for the annulene forms. The AI model based on benzene and Kekule benzene cannot be applied to homoaromatic systems, i.e. systems for which the $\pi$-delocalization is interrupted by one or more C atoms with 4 formal single bonds, as is the case of **1b** and **2b**.

**Analysis of crystal packing effects.** To test the possibility of the unusual $R$ value of **1** being the result of crystal packing effects, two different situations were considered. (i) In the unit cell of **1**, one molecule sits beside the other.[44] We considered the interactions between molecules in different unit cells, especially that situation where one molecule sits on top of the other, slightly shifted. Steric repulsion caused by packing effects could force the widening of the external C12−C11−C13 bridge angle $\beta$, and with this widening the $R$ value could be forced to decrease. Therefore, the changes in $R$ were calculated for $\beta$ values from 102 to 120°; that is, geometry optimizations were carried out for a series of fixed $\beta$ values. (ii) Utilizing the crystal data, the dimer geometry was optimized under the constraint that the distance between the monomers and the relative orientation to each other does not change. Under the same conditions, $R$ was fixed for one monomer and the geometry of the dimer reoptimized. (iii) A tetramer defined by the crystal structure was analyzed under the conditions described in (ii).

The quantum chemical calculations were performed with the program packages MOLPRO,[87] COLOGNE14,[88] CFOUR,[89] and Gaussian.[90]

## 3. RESULTS AND DISCUSSION

In Figure 2, the calculated PECs for a representative number of the different methods applied in this work are shown. The most accurate enthalpy and free energy curves, $\Delta H(R)$ = PHC and $\Delta G(R)$ = PGC, respectively, are given in Figure 3. Relative energies $\Delta E$, $\Delta H(298)$, and $\Delta G(298)$ obtained at different levels of theory are listed in Table 1. In Figures 2 and 3, $\Delta E = 0$ or $\Delta H(298) = 0$ was arbitrarily chosen for $R = 2.1$ Å. In Table 1, the reference point of all energy difference determinations is always the most stable annulene form. However, when one of the target geometries was located on a shoulder of the PEC (or the corresponding PHC and PGC), the $R$ value of the inflection point or the $R$ of the annulene (bisnorcaradiene) minimum of a closely related method was taken, as is indicated in Table 1. In Figure 4, some representative geometries of **1** and the reference molecules investigated in this work are shown.

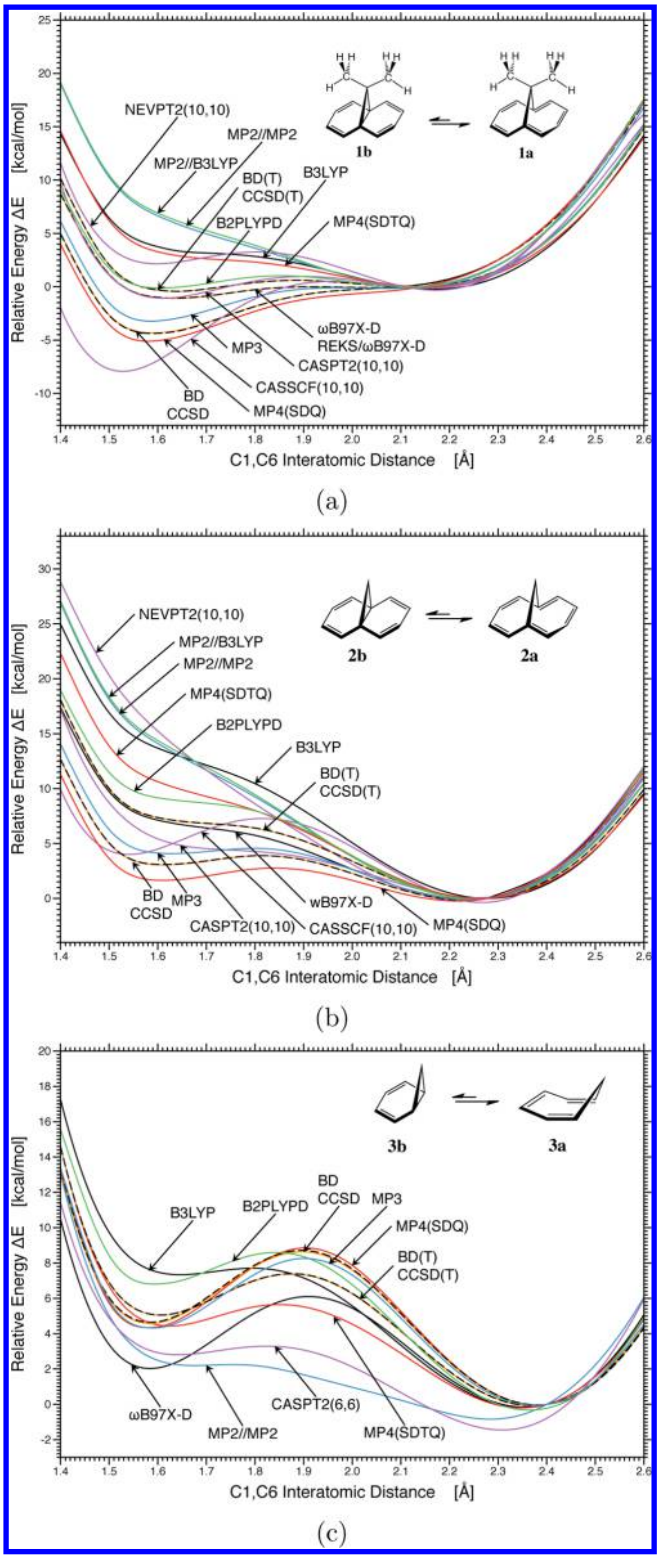


**Figure 2.** Representation of the energy changes as a function of the 1,6-distance $R$ of (a) 11,11-dimethyl-1,6-methano[10]annulene (**1a**), (b) 1,6-methano[10]annulene (**2a**), and (c) 1,3,5-cycloheptatriene (**3a**) obtained at multiple levels of theory. For **1** and **2**, $R$ values of 2.1 and 2.25 Å have been used to determine the energy zero level, thus facilitating the comparison.


dx.doi.org/10.1021/jp5082966 | J. Phys. Chem. A 2015, 119, 1666−1682

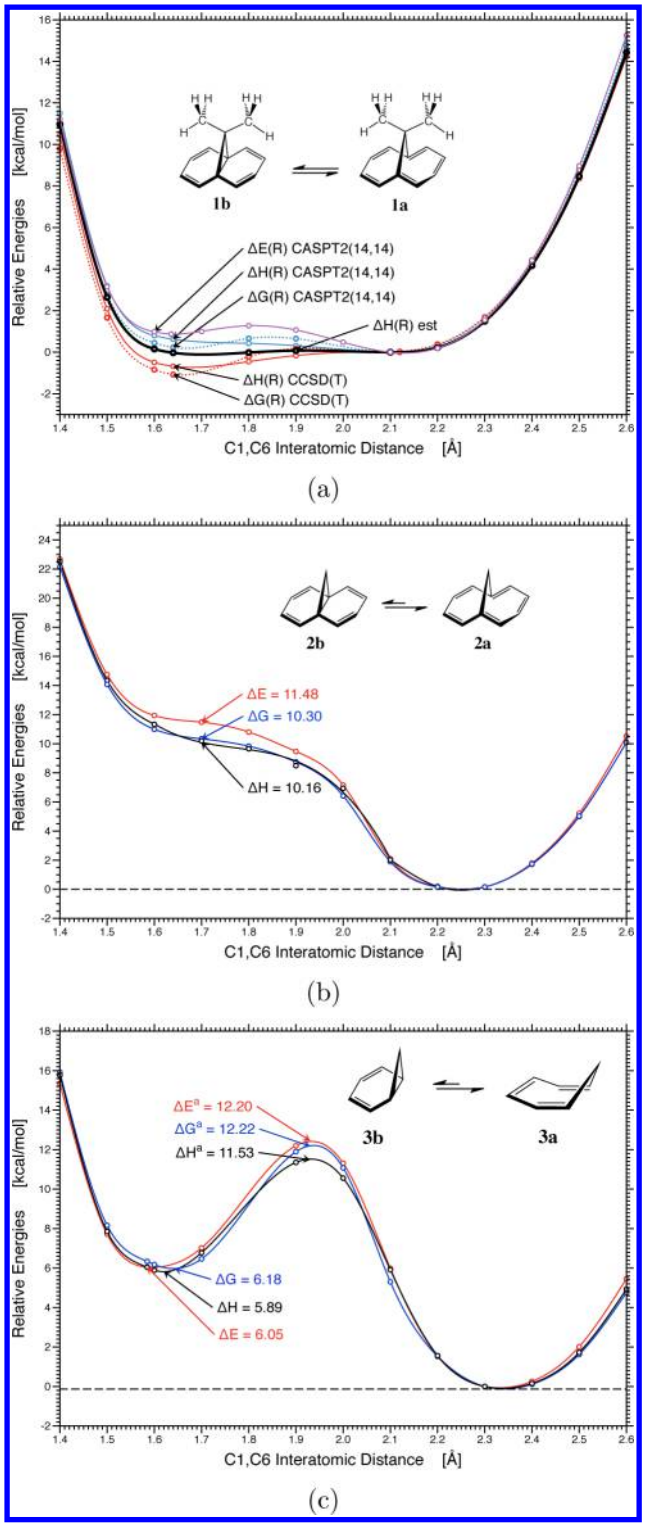


**Figure 3.** Representation of energy, enthapy, and free energy changes as a function of the 1,6-distance $R$ of (a) 11,11-dimethyl-1,6-methano[10]annulene (**1a**), (b) 1,6-methano[10]annulene (**2a**), and (c) 1,3,5-cycloheptatriene (**3a**). Potential energy curves in (a) are obtained at the CASPT2(14,14) and CCSD(T) levels of theory. For estimated (est) curves, see text. Potential energy curves in (b) and (c) are determined at CASPT2(14,14) and CASPT2(10,10) levels of theory. See text.

In the following, we will first analyze the PECs, PHCs, and PGCs obtained for target system **1**. The PECs calculated for **1** reveal that (i) $\pi$-electron delocalization in annulene and bisnorcaradiene, (ii) $\sigma-\pi$ interactions in the distorted ring perimeter, (iii) homoaromatic through-bond and through-space interactions (as defined by Cremer and co-workers[10]), (iv) the generation of a biradicaloid and its stabilization by electron delocalization, (v) strain effects in the bisnorcardiene form, and (vi) bridge−ring interactions have to be considered as important electronic effects. Different methods account for these effects in different ways so that the PEC adopts either a single well (SW) form, a SW with a shoulder at small or large $R$ values (SW + 1S or SW + 2S), as well as a double-well (DW) with a flat minimum for small $R$ (DW-F1M) or large $R$ (DW-F2M).

Details of the analysis of the PECs for the different WFT and DFT methods, especially their account of dynamical and nondynamical electron correlation effects, are given in the Supporting Information. Despite the testing of a large number of different WFT and DFT methods (more than 20 as shown in Table 1 and Figure 2a), none of them provides a balanced account of effects (i) to (vi), and none of the results is in line with experimental observations made for **1**. Therefore, the question remains whether other effects such as thermochemical corrections, entropy contributions, crystal packing, or solvent effects may improve the agreement between theory and experiment. Rather than investigating these possibilities first, we pursue an alternative way, which leads to the description of the smaller, closely related valence tautomeric systems **2** and **3**, for which all experimental information available implies the existence of a SW potential (**2**)[25,34,47,49] or a DW potential favoring the no-bond form **3a** (**3**),[91−94] which should be much easier to describe.

**Valence tautomerism of 1,6-methano[10]annulene and cycloheptatriene.** Extensive spectroscopic and diffraction measurements were carried out in the case of **2**.[25,34,47,49] The difference between **2a** (being more stable) and **2b** was estimated to be ≤10 kcal/mol. All measured NMR, infrared, Raman, or UV values exclude a second minimum for the bisnorcaradiene form **2b**. Hence, a SW+1S form of the PEC is most likely.[25,34,47,49]

In the case of the cycloheptatriene−norcaradiene system **3**, a DW PEC has been verified by both NMR and kinetic studies.[91,93] Experiments conducted by Rubin[93] led to a free activation energy for the transition **3b** → **3a** of $\Delta G^{a}(298) = 7.2$ kcal/mol. Rubin estimated $\Delta G(298, \mathbf{3b})$ to be $4 \pm 2$ kcal/mol, which implies $\Delta G^{a}(298, \mathbf{3a} \rightarrow \mathbf{3b}) = 11 \pm 2$ kcal/mol where a zero-entropy change was assumed.[93] The estimates were based on the NMR results of Gorlitz and Günther, who estimated that **3b** should have a finite concentration of 0.1% at room temperature.[91] In this work, we find the concentration of **3b** to be just 0.003%.

As in the case of **1**, most of the methods applied failed to provide PECs and relative energies that are in line with these experimental observations (see Tables 2 and 3 as well as Figure 2b and 2c), where the rationalization of these shortcomings in terms of dynamical and nondynamical electron correlation effects are similar to those given for **1**. $\omega$B97X-D, CCSD(T), BD(T), MP4(SDTQ), and B2PLYPD lead to reasonable PECs for **2**, suggesting that the bisnorcaradiene form **2b** is located on a shoulder of the PEC. However, only MP4(SDTQ) and B2PLYPD provide a relative energy of **1b** close to 10 kcal/mol, whereas especially CASPT2(10,10), CCSD(T), and BD(T) severely underestimate the destabilization of **2b**. Especially, the PEC of CASPT2(6,6) leads to a rearrangement barrier **3a** →


dx.doi.org/10.1021/jp5082966 | J. Phys. Chem. A 2015, 119, 1666−1682

Table 1. Relative Energies and Rearrangement Barriers of 11,11-Dimethyl-1,6-methano[10]annulene

| Method | Curve[a] | $R$(1b)[b] | $R$(1a) | $\Delta E$(1b)[c] | $\Delta E(TS)$[d] |
|---|---|---|---|---|---|
| HF | SW+2S | 1.552 | (2.120) | −9.29 | |
| SVWN5 | SW+1S | (1.640) | 2.125 | 3.26 | |
| BLYP | SW+1S | (1.640) | 2.212 | 6.99 | |
| B97 | SW+1S | (1.685) | 2.134 | 2.84 | |
| B3LYP | SW+1S | (1.640) | 2.167 | 3.67 | |
| $\omega$B97 | SW+2S | 1.595 | (2.040) | −7.03 | |
| $\omega$B97X | SW+2S | 1.595 | (2.040) | −4.28 | |
| $\omega$B97X-D | DW-F2M | 1.638 | 2.039 | −1.02 | 0.07 (1.09) |
| REKS/$\omega$B97X-D | DW-F2M | 1.637 | 2.039 | −0.98 | 0.07 (1.05) |
| B2P-LYP-D | DW-F2M | 1.605 | 2.118 | −0.08 | 1.05 (1.13) |
| MP2 | SW+1S | (1.640) | 2.154 | 6.31 | |
| MP3 | DW-F2M | 1.587 | 2.065 | −3.10 | 0.04 (3.14) |
| MP4(SDQ) | SW+2S | 1.581 | (2.120) | −5.28 | |
| MP4(SDTQ) | SW+1S | (1.640) | 2.150 | 2.92 | |
| CCSD | SW+1S | 1.590 | (2.120) | 4.25 | |
| BD | SW+1S | 1.590 | (2.120) | 4.21 | |
| CCSD(T) | DW-F2M | 1.641 | 2.120 | −0.42 | 0.62 (1.04) |
| BD(T) | DW-F2M | 1.641 | 2.120 | −0.42 | 0.62 (1.04) |
| CASSCF(10,10) | DW-F2M | 1.529 | 2.148 | −7.81 | 0.63 (8.44) |
| CASPT2(10,10) | DW-F2M | 1.613 | 2.159 | −0.97 | 1.07 (2.04) |
| NEVPT2(10,10) | DW-F1M | 1.598 | 2.172 | 2.49 | 3.59 (1.10) |
| CASPT2(14,14) | DW-F1M | 1.647 | 2.130 | 0.91 | 1.32 (0.41) |
| Estimate | DW-F2M | 1.643 | 2.123 | 0.26 | 0.93 (0.67) |
| | | | | $\Delta H$(**1b**) | $\Delta H$(TS) |
| B2P-LYP-D | DW-F2M | 1.694 | 2.110 | 0.61 | 1.14 (0.53) |
| CCSD(T) | DW-F2M | 1.680 | 2.120 | −0.68 | 0.03 (0.71) |
| BD(T) | DW-F2M | 1.684 | 2.120 | −0.75 | 0.02 (0.77) |
| CASPT2(14,14) | DW-F1M | 1.640 | 2.120 | 0.66 | |
| Estimate | DW-F2M | 1.662 | 2.125 | −0.11 | 0.08 (0.19) |
| | | | | $\Delta G$(**1b**) | $\Delta G$(TS) |
| B2P-LYP-D | DW-F2M | 1.680 | 2.114 | 0.16 | 0.83 (0.67) |
| CCSD(T) | DW-F2M | 1.658 | 2.080 | −1.09 | 0.20 (1.29) |
| BD(T) | DW-F2M | 1.658 | 2.120 | −1.12 | 0.19 (1.31) |
| CASPT2(14,14) | DW-F1M | 1.665 | 2.120 | 0.22 | 0.73 (0.51) |
| Estimate | DW-F2M | 1.662 | 2.100 | −0.45 | 0.42 (0.87) |

[a]Curve indicates the shape of the rearrangement potential. DW-F1M, double well with flat first minimum; DW-F2M, double well with flat second minimum; SW+1S, single well with shoulder at small $R$; SW+2S, single well with shoulder at large $R$. [b]$R$(**1b**) and $R$(**1a**) indicate the C1C6 distance for each structure in Å. Values in parentheses are approximate values to determine the position of the shoulder. [c]$\Delta E$(**1b**) gives the energy difference relative to **1a** in kcal/mol. For the explanation of the estimated values, see text. [d]$\Delta E(TS)$, $\Delta H(TS)$, and $\Delta G(TS)$ give the energy barriers for valence tautomerization from **1a** to **1b** in kcal/mol. Values in parentheses are for the reverse reactions.

**3b**, which is 4.8 kcal/mol, more than 6 kcal/mol below the estimated $\Delta G^a(298)$ of 11 kcal/mol.[93]

The CASPT2(6,6) results reveal that the active space chosen is too small to provide a reliable description of the valence tautomeric rearrangement. Previous work by Cremer and co-workers has emphasized the homoaromatic interactions of the two $\pi$-bonds of norcaradiene with the 3 $\sigma$ bonds of the cyclopropyl group.[62] Obviously, these are essential for a correct description of the process **3a** → **3b**. Accordingly, we enlarged the (6,6) to a (10,10) active space by including all 6 rather than just 2 Walsh orbitals of the cyclopropyl group. The result of this extension of the active space is stunning: The barrier increases to 12.2 kcal/mol, and the relative energy of norcaradiene **3b** adopts a value of 6.0 kcal/mol (Table 3).

Previous multireference investigations of **3** by Jarzeki and co-workers[95] led to different $\Delta E$ values (CASSCF: 21.6 kcal/mol; MROPT2 (multireference with perturbation corrections): 8.9 kcal/mol) because these authors used a (6,6) active space. Similarly, all single reference calculations provided poor results.[38,96] The CASPT2(10,10) results of this work, if converted into $\Delta G(298)$ with the help of B3LYP-calculated ZPE, entropy, and thermochemical corrections, lead to $\Delta G^a$(298,**3b** → **3a**) = 6.0 kcal/mol, in good agreement with the corresponding experimental value of 7.2 kcal/mol (6.1 kcal/mol at 110 K).[93] The deviation results from an exaggeration of $\Delta S^a$ by the experiment: −4.5 e.u. (derived from the Arrhenius $A$ factor) vs −1.3 e.u. calculated in this work. Rubin's other estimates are corrected by our calculated $\Delta G^a$(298, **3a** → **3b**) of 12.2 kcal/mol and the relative value of **3b**: $\Delta G^a$(298, **3b**) = 6.2 kcal/mol; that is, they show that just 0.003% of **3b** are in equilibrium with **3a** at room temperature, where the previous 0.1% estimate was based on NMR experiments.[91] The potential curve obtained for $\Delta H(298)$ is shown in Figure 3c and probably presents the most accurate


dx.doi.org/10.1021/jp5082966 | J. Phys. Chem. A 2015, 119, 1666−1682

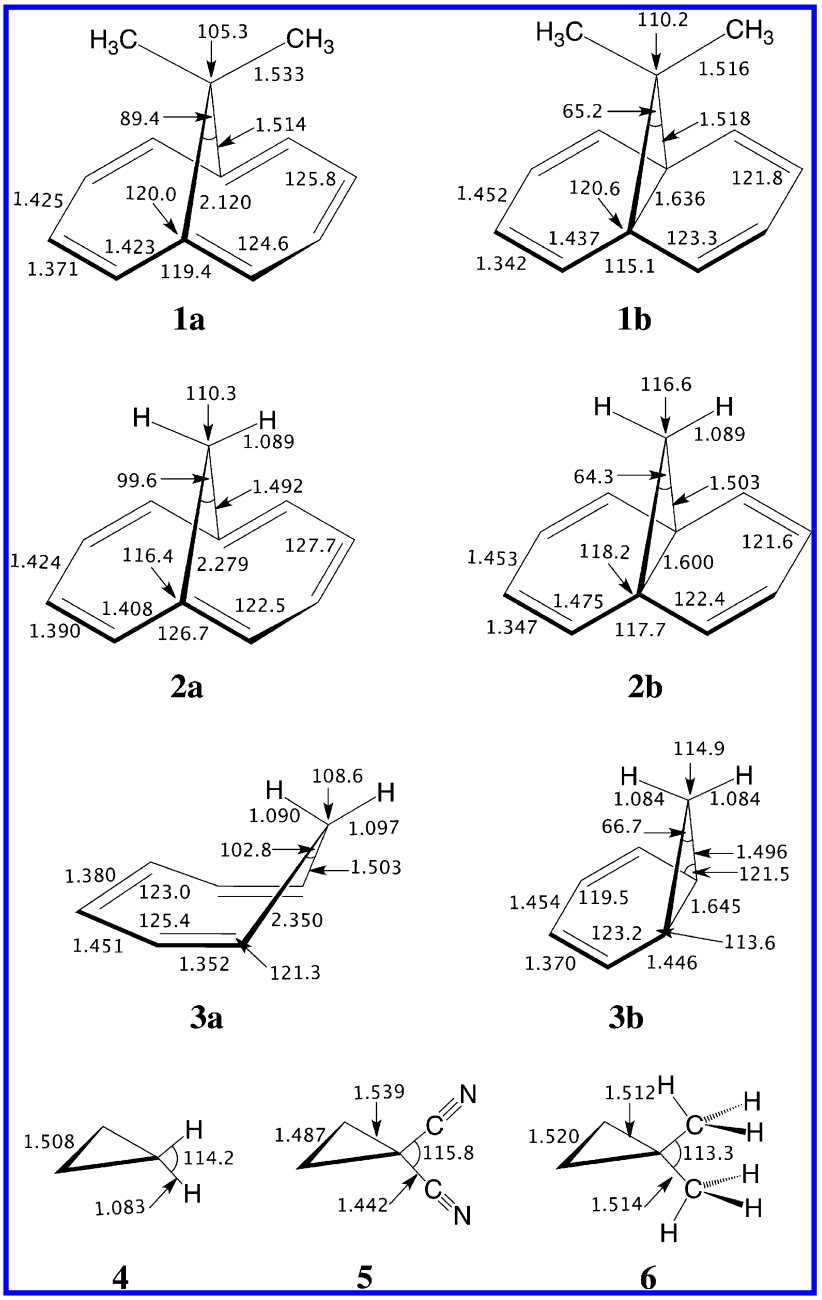


**Figure 4.** B3LYP geometries of **1**−**6**. Bond lengths in Å and bond angles in degrees.

description of the energetics of the valence tautomeric system **3** obtained so far.

Based on the experience earned for **3**, we extended the (10,10) active spaces of **1** and **2** to (14,14) spaces, which include the C1C11 and C1C6 $\sigma$ and $\sigma^*$-orbitals (Walsh orbitals). Here we discuss first the results for **2**. The PEC is still obtained in a SW+1S form where **2b** is now 11.5 rather than 5.3 kcal/mol higher in energy than the annulene form at the potential minimum at $R$ = 2.256 Å (X-ray: 2.235 Å[25]). The corresponding $\Delta H(298)$ and $\Delta G(298)$ values are 10.2 and 10.3 kcal/mol, respectively, in line with experimental observations.[24−27,29−31,33−35,37,47,48] Clearly, **2** has to be considered as [10]annulene rather than a bicyclic, homoaromatic $\pi$-system because $R$ = 2.256 Å is too large to lead to sizable through-space interactions.[10]

These results show clearly that CCSD(T) and BD(T), although they may account for some nondynamical effects besides the dynamical electron correlation effects, fail to describe the TS region and **3b** correctly, which can also be observed for **2b**, as too much stability is assigned to the norcaradiene forms. Therefore, we repeated the CASPT2 calculations for **1** with the larger (14,14) active space.

**Revised CASPT2 results and the consideration of thermochemical corrections.** CASPT2(14,14) leads to a PEC where the relative energies of **1a** and **1b** are interchanged compared to the CASPT2(10,10) PEC; that is, **1a** becomes the minimum of a relatively flat potential (0.91 kcal/mol below **1b**) with barriers of 1.32 and 0.41 kcal/mol for the valence tautomeric rearrangement (Table 1). Small changes in the ZPE and thermal correction values lead to a slight stabilization of **1b** and a vanishing of the rearrangement barrier for the PHC (see


dx.doi.org/10.1021/jp5082966 | J. Phys. Chem. A 2015, 119, 1666−1682

Table 2. Relative Energies and Rearrangement Barriers of 1,6-Methano[10]annulene

| Method | Curve[a] | $R$(**1b**)[b] | $R$(**1a**) | $\Delta E$(**1b**)[c] | $\Delta E(TS)$[d] |
|---|---|---|---|---|---|
| HF | DW-F1M | 1.562 | 2.219 | 0.63 | 3.27 (2.64) |
| B3LYP | SW+1S | (1.610) | 2.280 | 13.60 | |
| ωB97 | DW-F2M | 1.560 | 2.226 | −1.12 | 1.48 (2.60) |
| ωB97X | DW-F1M | 1.546 | 2.226 | 2.71 | 3.39 (0.68) |
| ωB97X-D | SW+1S | (1.610) | 2.240 | 7.22 | |
| B2P-LYP-D | SW+1S | (1.610) | 2.250 | 9.22 | |
| MP2 | SW+1S | (1.610) | 2.254 | 13.93 | |
| MP3 | DW-F1M | 1.630 | 2.240 | 4.20 | 4.68 (0.48) |
| MP4(SDQ) | DW-F1M | 1.610 | 2.214 | 1.88 | 3.00 (1.12) |
| MP4(SDTQ) | SW+1S | (1.610) | 2.265 | 10.48 | |
| CCSD | DW-F1M | 1.613 | 2.235 | 3.21 | 4.04 (0.83) |
| BD | DW-F1M | 1.612 | 2.234 | 3.25 | 4.06 (0.81) |
| CCSD(T) | SW+1S | (1.610) | 2.254 | 7.29 | |
| BD(T) | SW+1S | (1.610) | 2.256 | 7.32 | |
| CASSCF(10,10) | DW-F1M | 1.540 | 2.268 | 4.37 | 7.65 (3.28) |
| CASPT2(10,10) | SW+1S | (1.610) | 2.254 | 5.32 | |
| NEVPT2(10,10) | SW+1S | (1.610) | 2.230 | 14.86 | |
| CASPT2(14,14) | SW+1S | (1.700) | 2.256 | 11.48 | |
| | | | | $\Delta H$(**1b**) | $\Delta H$(TS) |
| B2P-LYP-D | SW+1S | (1.610) | 2.267 | 12.59 | |
| CCSD(T) | SW+1S | (1.700) | 2.256 | 5.60 | |
| BD(T) | SW+1S | (1.700) | 2.258 | 5.55 | |
| CASPT2(14,14) | SW+1S | (1.700) | 2.256 | 10.16 | |
| | | | | $\Delta G$(**1b**) | $\Delta G$(TS) |
| B2P-LYP-D | SW+1S | (1.610) | 2.267 | 12.23 | |
| CCSD(T) | SW+1S | (1.700) | 2.256 | 5.77 | |
| BD(T) | SW+1S | (1.700) | 2.258 | 5.74 | |
| CASPT2(14,14) | SW+1S | (1.700) | 2.256 | 10.30 | |

[a]Curve indicates the shape of the rearrangement potential. DW-F1M, double well with flat first minimum; DW-F2M, double well with flat second minimum; SW+1S, single well with shoulder at small $R$; SW+2S, single well with shoulder at large $R$. [b]$R$(**2b**) and $R$(**2a**) indicate the C1C6 distance for each structure in Å. Values in parentheses are approximate values to determine the position of the shoulder. [c]$\Delta E$(**2b**) gives the energy difference relative to **2a** in kcal/mol. For the explanation of the estimated values, see text. [d]$\Delta E(TS)$, $\Delta H(TS)$, and $\Delta G(TS)$ give the energy barriers for valence tautomerization from **2a** to **2b** in kcal/mol. Values in parentheses are for the reverse reactions.

Figure 3a). For CCSD(T) and BD(T), the conversion into enthalpies has a similar effect on the potential (Table 1). Considering that ZPE and thermochemical corrections are based in this work on harmonic frequencies, which may change differently with $R$ than anharmonically corrected frequencies, we recalculated all vibrational corrections with scaled frequencies employing the scaling factors suggested by Scott and Radom[97] for DFT. However, no significant changes were obtained in this way.

As mentioned above, even a (14,14) active space may not be sufficient to describe all nondynamical electron correlation effects resulting from the interactions of σ- and π-electrons, the stabilizing interactions in the intermediate biradicals, and the bridge−ring interactions. Apart from this, the amount of dynamical electron correlation provided by CASPT2 is much too small and biased to prefer the annulene. Conversely, CCSD(T) or BD(T) is not capable of correctly describing the nondynamical correlation. Since our computational possibilities do not provide a combination of these methods, we constructed a model PEC, PHC, and PGC by simply averaging the corresponding curves for CASPT2(14,14) and CCSD(T).

Although this model PHC (given in Figure 3a) may be considered to provide only a semiquantitative insight into the problem, it suggests a broad single well potential slightly preferring the bisnorcaradiene form by −0.1 kcal/mol (activation enthalpies: 0.1 and 0.2 kcal/mol). The $\Delta G(R)$ curve increases the preference of **1b** and introduces a somewhat stronger asymmetry of the potential (Figure 3a). Obviously, the degree of asymmetry of PHC and PGC increases with the admixture of an additional nondynamical electron correlation. Such a broad asymmetric SW potential would explain the observed strong $T$-dependence of the $^{13}C$ chemical shifts of **1** (they indicate a stronger population of the annulene form at higher $T$[49,50]) and the fact that **1** adopts in the unit cell two different forms probably influenced by crystal packing effects ($R$ = 1.836 and 1.780 Å[44]). Therefore, we will investigate environmental influences on the PECs, PHCs, and PGCs shown in Figures 2a and 3a in the following subsection.

**Consideration of solvent and crystal packing effects.** The dipole moment of annulene **1a** is 0.35 D at $R$ = 2.03 and 0.11 D for $R$ = 1.638 Å (ωB97X-D calculations), where the orientation is along the $C_2$ axis (bridge, positively charged; center of the perimeter, negatively charged). There is a charge transfer from the $CMe_2$ bridge to the annulene perimeter, which changes, in agreement with the changes in the dipole moment, from 13 ($R$ = 2.039 Å) to 9 me (millielectrons; $R$ = 1.638 Å).


dx.doi.org/10.1021/jp5082966 | J. Phys. Chem. A 2015, 119, 1666−1682

Table 3. Relative Energies and Rearrangement Barriers of 1,3,5-Cycloheptadiene and Norcaradiene

| Method | Curve[a] | $R$(**3b**)[b] | $R$(**3a**) | $\Delta E$(**3b**)[c] | $\Delta E(TS)$[d] |
|---|---|---|---|---|---|
| HF | DW-F1M | 1.557 | 2.395 | 7.03 | 12.70 (5.67) |
| B3LYP | DW-F1M | 1.644 | 2.351 | 7.51 | 7.89 (0.38) |
| $\omega$B97 | DW-F2M | 1.576 | 2.366 | −0.80 | 5.43 (6.23) |
| $\omega$B97X | DW-F1M | 1.576 | 2.350 | 2.18 | 6.14 (3.96) |
| $\omega$B97X-D | DW-F1M | 1.585 | 2.355 | 2.20 | 6.28 (4.08) |
| B2P-LYP-D | DW-F1M | 1.594 | 2.364 | 7.13 | 8.92 (1.79) |
| MP2 | DW-F1M | 1.675 | 2.286 | 3.02 | 3.07 (0.05) |
| MP3 | DW-F1M | 1.591 | 2.373 | 4.38 | 8.31 (3.93) |
| MP4(SDQ) | DW-F1M | 1.582 | 2.385 | 4.37 | 8.89 (4.52) |
| MP4(SDTQ) | DW-F1M | 1.623 | 2.341 | 4.64 | 5.85 (1.21) |
| CCSD | DW-F1M | 1.583 | 2.382 | 4.69 | 8.76 (4.07) |
| BD | DW-F1M | 1.585 | 2.380 | 4.62 | 8.68 (4.06) |
| CCSD(T) | DW-F1M | 1.607 | 2.370 | 4.99 | 7.33 (2.34) |
| BD(T) | DW-F1M | 1.607 | 2.366 | 5.10 | 7.34 (2.24) |
| CASPT2(6,6) | DW-F1M | 1.633 | 2.310 | 4.36 | 4.84 (0.48) |
| CASPT2(10,10) | DW-F1M | 1.593 | 2.334 | 6.05 | 12.20 (6.15) |
| | | | | $\Delta H$(**1b**) | $\Delta H$(TS) |
| B2P-LYP-D | DW-F1M | 1.653 | 2.245 | 6.33 | 6.34 (0.01) |
| CCSD(T) | DW-F1M | 1.738 | 2.476 | 4.95 | 6.92 (1.97) |
| BD(T) | DW-F1M | 1.738 | 2.476 | 4.96 | 6.93 (1.97) |
| CASPT2(10,10) | DW-F1M | 1.641 | 2.334 | 5.89 | 11.53 (5.64) |
| | | | | $\Delta G$(**1b**) | $\Delta G$(TS) |
| B2P-LYP-D | DW-F1M | 1.697 | 2.245 | 6.47 | 6.64 (0.17) |
| CCSD(T) | DW-F1M | 1.698 | 2.482 | 5.35 | 7.62 (2.27) |
| BD(T) | DW-F1M | 1.698 | 2.482 | 5.34 | 7.59 (2.25) |
| CASPT2(10,10) | DW-F1M | 1.618 | 2.334 | 6.18 | 12.22 (6.04) |

[a]Curve indicates the shape of the rearrangement potential. DW-F1M, double well with flat first minimum; DW-F2M, double well with flat second minimum; SW+1S, single well with shoulder at small $R$; SW+2S, single well with shoulder at large $R$. [b]$R$(**3b**) and $R$(**3a**) indicate the C1C6 distance for each structure in Å. [c]$\Delta E$(**3b**) gives the energy difference relative to **3a** in kcal/mol. For the explanation of the estimated values, see text. [d]$\Delta E(TS)$, $\Delta H(TS)$, and $\Delta G(TS)$ give the energy barriers for valence tautomerization from **3a** to **3b** in kcal/mol. Values in parentheses are for the reverse reactions.

Experimental work with **1** was carried out in nonpolar solvents such as cyclohexane, $CS_2$, $CCl_4$, or methanol.[23,34,50] Therefore, we calculated the solvent influence by increasing the dielectric constant $\epsilon$ from 2 to 32.7[66] and using Tomasi's PCM method.[65] In all calculations, changes in the relative free energies $\Delta G(298)$ were 0.1 kcal/mol or smaller, always in favor of the annulene form (in line with the calculated dipole moments), which in the case of the estimated potential of Figure 3a (see also Table 1) would decrease the $\Delta G(298)$ difference between **1a** and **1b** and lead to a larger population of the annulene form with increasing $T$, as found in the NMR experiments.[49,50] Hence, environmental effects cannot be ignored if free energy differences smaller than RT = 0.6 kcal/mol have to be discussed.

There is also the possibility that the unusual C1C6 distances observed in the crystal structure analysis[44] are the result of packing effects. In this connection, it has to be pointed out that strings of molecules **1** arranged in parallel form molecular sheets.[44] Molecules which are on top of each other in different sheets could, via exchange repulsion, widen the external C12C11C13 bridge angle, thus causing stronger bridge−perimeter interactions. As is shown in Figure 5, the downward oriented methyl hydrogens are just 1.96−2.15 Å away from the center of the C3C4 and C8C9 bond, respectively. Considering that these H atoms carry a small positive charge and that the sum of the van der Waals distances for H and C is 1.2 + 1.6 = 2.8 Å,[66] the downward oriented methyl H atoms should be attracted by the $\pi$-density of the [10]annulene perimeter. There is a stabilizing H−$\pi$ interaction at a distance of 2.4 Å, which is qualitatively confirmed by the increase in the stabilization of the annulene form when comparing $\omega$B97X-D and $\omega$B97X results (see Supporting Information).

The hypothesis of an increased bridge−perimeter attraction caused by bridge angle widening in the course of crystal state packing effects was confirmed as a widening of the CCC-bridge angle had a significant impact on the parameter $R$: Widening the bridge angle C12C11C13 by 10° leads to an increase in $R$ by 0.048 Å.

Next, we calculated the geometry of the dimer and the tetramer shown in Figure 5 by applying a constrained optimization, in which the distance(s) between the monomers and the relative orientation to each other were frozen ($\omega$B97X-D calculations). The differences in the monomer geometries are small for the dimer ($R$: 1.635 for the lower monomer; 1.631 Å for the upper monomer). However, for the tetramer, $R$ values of 1.636 (top, left), 1.642 (top, right), 1.637 (bottom, left), and 1.619 Å (bottom, right) are obtained, leading to a total variation of 0.023 Å. These changes are in line with the X-ray diffraction result ($\Delta R$ in the unit cell: 0.056 AA[44]) where one has to consider that only the lower right monomer (the one with the short $R$) has an environment close to that which it would have in the solid state. For reproducing the experimental


dx.doi.org/10.1021/jp5082966 | J. Phys. Chem. A 2015, 119, 1666−1682

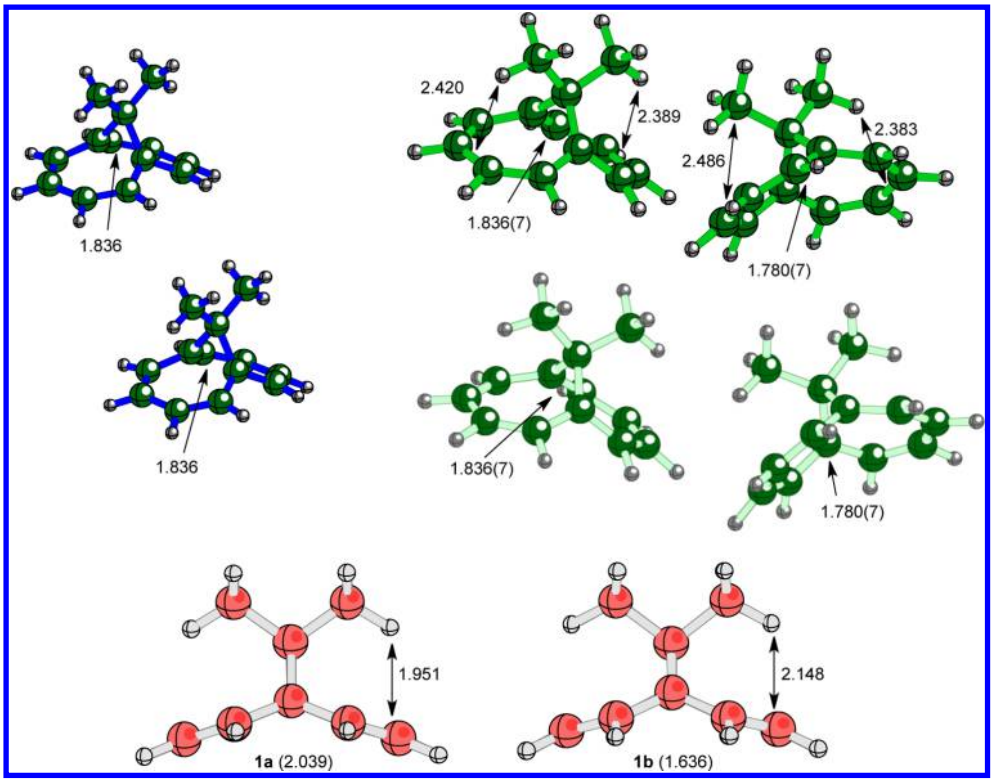


**Figure 5.** Dimer and tetramer configurations that were calculated to investigate crystal packing effects. The green structures give a tetramer of **1** and show how two unit cells are arranged in the crystal.[44] The blue structures on the left show the arrangement for the dimer of **1** that was calculated in the search for packing effects. The red structures give for the ωB97X-D optimized geometry of **1a** and **1b** the shortest hydrogen-to-ring distances. See text.

situation, a more realistic model comprising at least 16 monomers (12 monomers surrounding a tetramer) at fixed distances and orientations would be needed. Apart from this, one has to consider that effects would become larger if ωB97X-D could correctly describe the asymmetric SW potential obtained at higher levels of WFT.

In another set of calculations, the dimer shown on the left side of Figure 5 (with frozen distance and relative orientation of the monomers) was optimized for fixed $R$ ($1.6 < R < 2.2$ Å) values of either the upper or the lower monomer, and optimizing the remaining geometrical parameters. For all these geometry optimizations, $R$ of the second monomer changed maximally by 0.005 Å relative to the corresponding monomer value where especially the positions of the methyl H atoms were sensitive. We conclude that, in view of the broad asymmetric SW potential calculated and the results obtained for the tetramer, crystal packing effects have an impact on $R$ and explain the existence of two molecules of **1** with different geometries in the unit cell.

**NMR investigation and an independent determination of the equilibrium geometry of 1.** In previous work, one of us has shown how an easily changing geometrical parameter of a flexible system can be determined in solution with the help of measured and calculated chemical shifts.[74,75] In Figure 6a, calculated $^{13}$C and $^{1}$H chemical shift values are given as a function of $R$ and compared with the available $^{13}$C chemical shifts indicated as dashed horizontal lines. Examination of this figure reveals that the shift value of C1 is the most sensitive. This shift increases from a typical value for vinyl cyclopropane (42.5 ppm[98]) to that found for **2a** (114.6 ppm[98]) and directly reflects the changes in $R$. At $R$ = 1.763 Å, the calculated C1 value becomes equal to the measured one, thus suggesting that this $R$ value is the one **1** adopts in solution or, alternatively, corresponds to a time-averaged value if the valence-tautomeric rearrangement of **1** is fast on the NMR time-scale.

A similar observation can be made for the NMR chemical shift of C11, which increases from a value typical of a cyclopropane ($^{13}$C shift: −2.8 ppm[98]) to the one measured for **2a** (34.8 ppm[98]) crossing the observed C11 shift at $R$ = 1.782 Å. The chemical shifts of the methyl carbon nuclei coincide at 1.865 Å with the corresponding measured value. However, these $^{13}$C shifts are less sensitive, as are those of C2 (coincidence at $R$ = 1.788 Å) and C3 (coincidence at $R$ = 2.168 Å, Figure 6a). The mean deviation Δ between measured and calculated $^{13}$C chemical shifts for the C atoms of the perimeter adopts a minimum at $R$ = 1.775 Å, as is shown in Figure 6. NMR chemical shift calculations are normally less accurate for conjugated systems, especially if these are nonplanar (the shifts of C2 and C3 are close to the experimental ones in the whole range $1.7 < R < 2.2$ Å, and a specific $R$ value is difficult to determine). We note that when C11, C12, C13, C1, and C6 are used for the comparison with experiment, a value of $R$ = 1.79 Å results, in good agreement with the X-ray diffraction values of $R$, which are close to 1.8 Å.[44]

The bisnorcaradiene and the annulene forms can both be excluded as clearly dominating the valence tautomeric rearrangement of **1** in the sense of a DW potential. The remaining possibility is a rapid rearrangement in solution via a small barrier of a DW potential or, more likely in view of our calculations, a broad asymmetric SW potential. This speaks for


dx.doi.org/10.1021/jp5082966 | J. Phys. Chem. A 2015, 119, 1666−1682

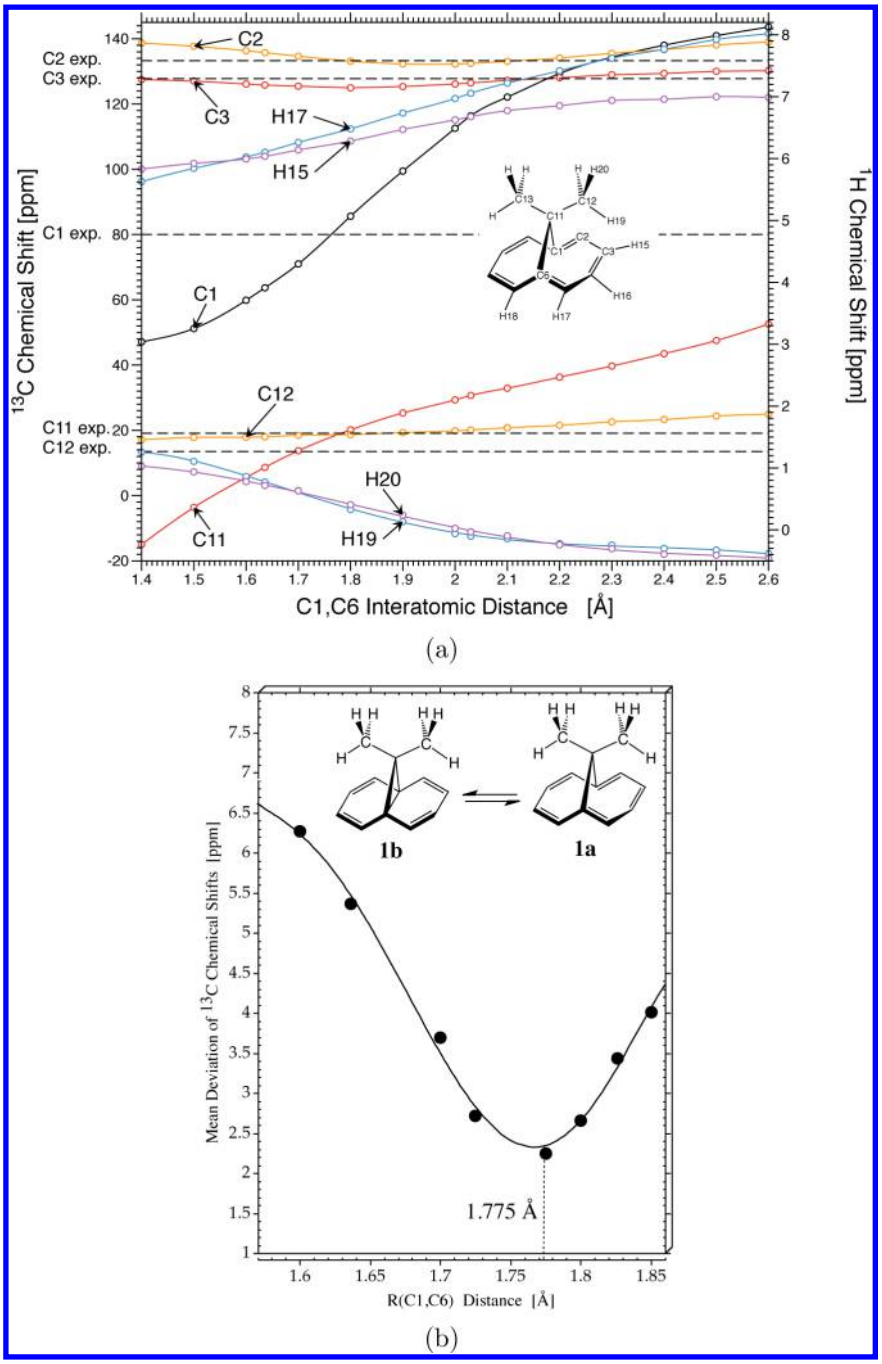


**Figure 6.** (a) Dependence of calculated NMR chemical shifts [ppm] of **1** on the distance $R$(C1C6) as calculated at the B3LYP/GIAO level of theory. (b) Mean absolute deviation [ppm] between measured and calculated $^{13}$C NMR chemical shifts of the ring carbon atoms given as a function of $R$.

a large-amplitude vibration in solution similar to the one suggested in Figure 3a.

Also informative in this connection are the calculated SSCCs $J(^{13}C^{13}C)$ and $J(^{1}H^{1}H)$ given as a function of $R$ (see Figure 7). When $R$ is close to 1.5 Å, the values of $^{1}J(C1C6)$ and $^{1}J(C1C11)$ adopt the values typical of cyclopropane (12.4 Hz[98]). For increasing $R$ the former $^{1}J$ value decreases to −12.4 Hz at 1.8 Å. This is comparable to the geminal $^{1}J(CC)$ value in a substituted cyclobutane (−8 Hz[98]) and then increases to a zero value at large $R$, indicating that through-bond or through-space coupling are small because the CCC-angle dependence of $^{2}J$ implies for this situation a zero value, $^{5}J$ coupling along the perimeter is too weak, and/or the C1C6 through-space overlap is too small. Hence, a measuring of $J(C1C6)$ (best in dependence of $T$) should provide an excellent possibility for an experimental determination of $R$.

Also informative should be the measurement of $^{1}J(C1C11)$, $^{1}J(C11C12)$, and $^{3}J(H15H16)$. The former $J$ value increases from about 16 Hz at $R$ = 1.60 Å to 28 Hz, typical of a $^{1}J(CC)$ value such as that of cyclobutane.[98] $^{1}J(C11C12)$ changes from 45 to 39 Hz for the same $R$ values while $^{3}J(H15H16)$ increases from 5.0 to 7.2 Hz. Since the changes in the $J(CC)$ values are larger, they should be preferably used for an independent determination of the $R$ value of **1** in solution.


dx.doi.org/10.1021/jp5082966 | J. Phys. Chem. A 2015, 119, 1666−1682

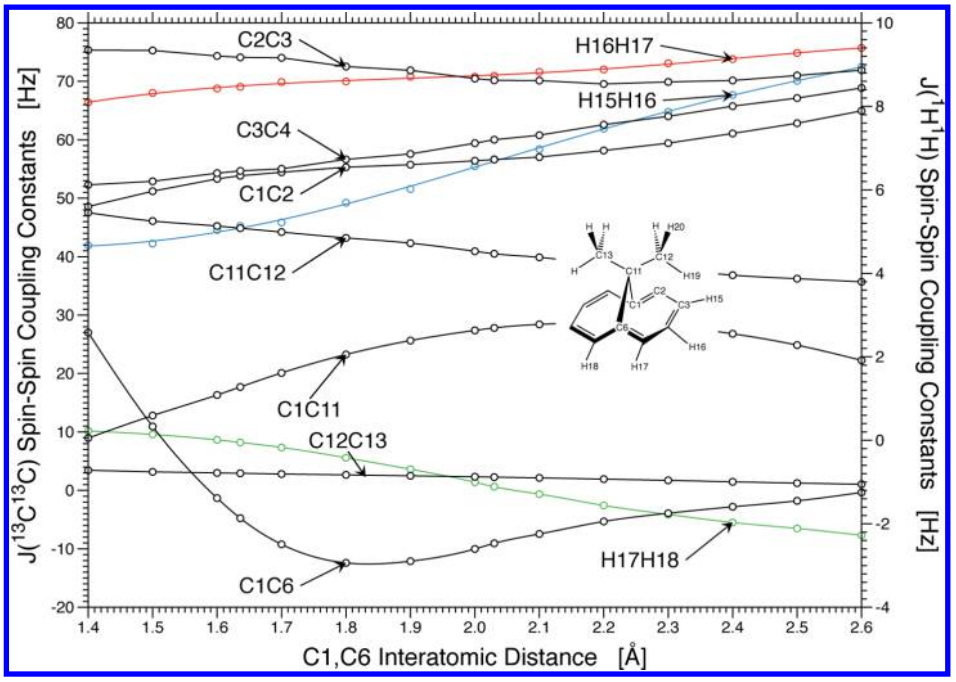


**Figure 7.** Dependence of calculated NMR spin−spin coupling constants $J$ [Hz] on $R$(C1,C6) of system **1**.

## 4. DOES 11,11-DIMETHYL-METHANO[10]ANNULENE POSSESS THE LONGEST CC BOND OF NEUTRAL CYCLOPROPYL DERIVATIVES?

System **1** is unusual because of its broad SW potential, which makes a large-amplitude C1C6 vibration possible, making a barrierless interconversion of the annulene into the bisnorcaradiene form possible. In this work, we clarified the question of the nature of the C1C6 interaction by two different model approaches utilizing the topological analysis of $\rho(\mathbf{r})$[69] in the way given by Cremer and Kraka[70,71,99] and the local vibrational mode approach of Cremer, Zou, and Konkoli.[77,80,100] In Figure 8, the BSO values $n$(CC) based on the calculated local CC stretching force constants are plotted as a function of $R$. For each set of local vibrational modes at a given $R$ value, the adiabatic connection scheme[80] is applied to determine whether a given local mode is still contained in a set of 3N-L modes directly related to the 3N-L normal vibrational modes. As can be seen from Figure 8, close to $R$ = 1.7 Å the C1C6 stretching mode drops out of the 3N-L set of vibrational modes, indicating that for larger $R$ values there is no C1C6 covalent bond.

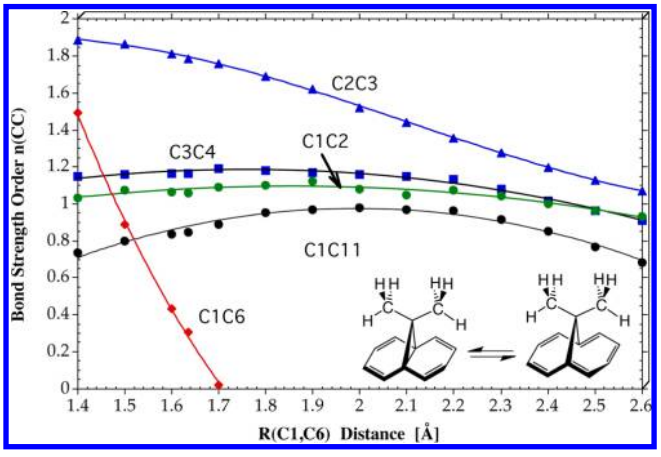


**Figure 8.** Bond strength orders $n$(CC) derived from local CC stretching force constants given as a function of $R$(C1,C6) of system **1**.

All other BSO(CC) values change smoothly from the bisnorcaradiene form to the annulene form where in the latter case the alternation of bonds is similar to that found for naphthalene;[81,86] that is, bonds C2C3, C4C5, etc. are the strongest, followed by bonds C3C4 and C8C9, whereas the weakest conjugated CC bonds sit at the bridge. The CC bridge bonds of **1b** are weaker than the normal CC bonds, with C1C6 being the weakest. The calculated AI of **1a** is 64% of the value obtained for benzene (100%), which is smaller than the value for **2a** (73%) and significantly smaller than the value for naphthalene (86%).[86] This is in line with the fact that **2a** and **3a** experience a strong perturbation of their 10$\pi$-perimeter caused by the 1,6-bridge leading to torsional angles up to 37°.

In Figure 9a, the changes in the bond critical and ring critical points $\mathbf{r}_b$ and $\mathbf{r}_r$ of the electron density distribution $\rho(\mathbf{r})$ are shown as a function of $R$. Some of the changes are similar and some are different from those given by the $n$(CC) based on the local CC stretching force constants (Figure 8). This is attributable to the fact that the electron density determined at one specific point in the bond region cannot reflect all the density changes taking place in the zero-flux surface between two bonded atoms apart from the influences of bond polarity, charge transfer, and other effects given by the changes in the virial (atomic) spaces of the molecule during a change in $R$. The local CC stretching force constants account for these effects and therefore are more reliable CC bond strength descriptors.

However, it is an accepted fact that covalent bonding requires the existence of a bond critical-point and zero-flux surface between the atoms in question and that the energy density at this bond critical point, $H(\mathbf{r}_b)$, must be stabilizing, i.e. smaller than zero (Cremer−Kraka criteria of covalent bonding).[70,71,99] This criterion is clearly fulfilled for all CC bonds and $R$ values of **1** investigated, except the C1C6 interaction, which converts into a noncovalent interaction at $R$


dx.doi.org/10.1021/jp5082966 | J. Phys. Chem. A 2015, 119, 1666−1682

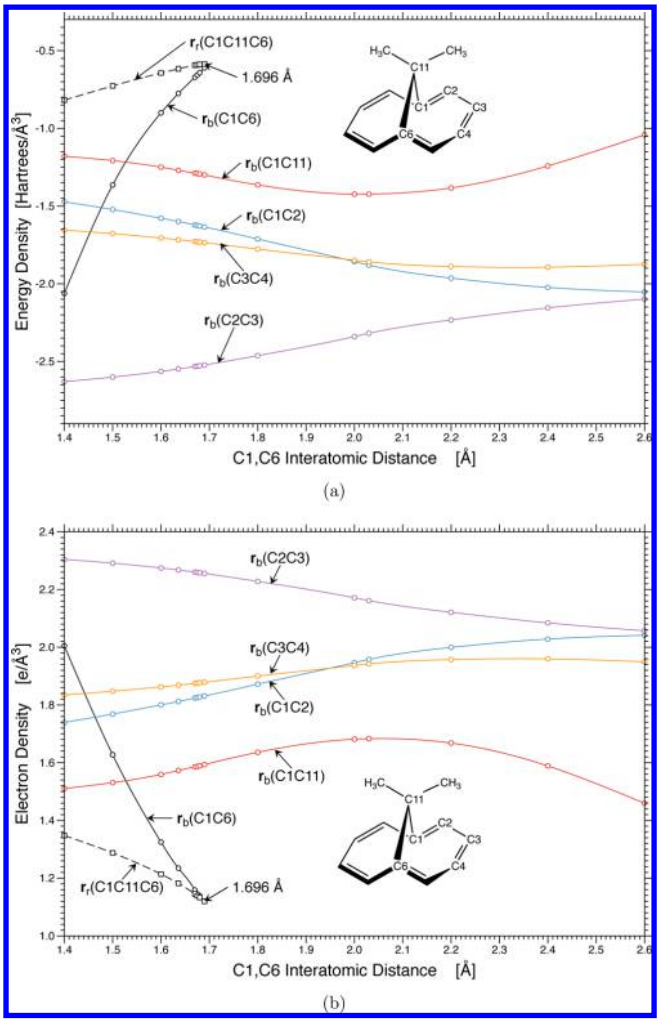


**Figure 9.** (a) Electron density $\rho(\mathbf{r})$ and (b) energy density $H(\mathbf{r})$ at bond critical and ring critical points given as a function of $R$(C1,C6) of system **1**.

= 1.696 Å. There the C1C6C11 ring critical point merges with the C1C6 bond critical point, thus leading to a singularity in the Hessian of $\rho(\mathbf{r})$ and the C1C6 maximum electron density path connecting these atoms vanishes. Applying the Cremer–Kraka criterion, there is no longer a covalent C1C6 bond for $R \geq 1.70$. This is in line with the independent observation made in connection with the local vibrational modes. We draw the conclusion that a C1C6 covalent bond with $R$ = 1.80 Å does not exist but that a homoaromatic interaction in the sense of a through-space overlap of $\pi$-orbitals exists leading to a small electron density increase between atoms C1 and C6.

**Impact of the bridge on the 10$\pi$-perimeter.** The electronic influence of electron-withdrawing and electron-donating substituents of a cyclopropane ring are well-known and has been amply described in the literature (for a review, see ref 62). Two cyano groups at C11 lead to a shortening of the distal bond (lengthening of the vicinal bonds; see **5** as compared to **4** in Figure 4), which has been exploited to synthesize 11,11-dicyano-bisnorcaradiene, i.e. the dicyano analogue of **1b**.[35] The effect of two methyl groups has been predicted to lead to a slight CC lengthening of the distal bond (slight shortening of the vicinal CC bonds)[62] as is confirmed by the bond lengths given for **6** in Figure 4. This indicates that dimethyl-substitution at C11 as in **1** should favor a larger rather than a smaller $R$, irrespective of any other stabilizing bridge–perimeter interactions.

The isodesmic energies for the formal reactions

$$\mathbf{4} + CH_3CH_2CH_3 \rightarrow \mathbf{6} + CH_4, \quad \Delta E = -3.78$$

$$\mathbf{2b} + CH_3CH_2CH_3 \rightarrow \mathbf{1b} + CH_4, \quad \Delta E = -3.38$$

$$\mathbf{2a} + CH_3CH_2CH_3 \rightarrow \mathbf{1a} + CH_4, \quad \Delta E = 4.92$$

(B3LYP values in kcal/mol) suggest a similar stabilization by the two methyl groups for cyclopropane and **2b** but a 5 kcal/mol destabilization for **2a**. The first two values are in line with a shortening of two vicinal and a lengthening of just one distal CC bond. Molecule **6** has a smaller external CCC angle than the HCH angle in its parent molecule (Figure 4), which is the result of steric repulsion between methyl groups and the ring. For the same reason, **1b** has an even smaller external angle (110.2°, Figure 4), where the folding back of the two diene units as shown in the side view at the bottom of Figure 5 leads to some reduction of the steric repulsion between methyl groups and the 6-membered rings. In the case of **1a**, steric attraction between methyl groups and the $\pi$-perimeter and steric repulsion (for **1a** the H-center(C3C4) distance is decreased from 2.148 to 1.951 Å, $\omega$B97X-D, see Figure 5) must be balanced, which leads to a small C12C11C13 angle (105.3°, Figure 4), methyl–methyl repulsion, and an overall destabilization, as reflected by the energy of the isodesmic reaction given above (4.9 kcal/mol).

The destabilizing effect of the $CMe_2$ bridge leads to a raising of the relative energy of **1a**. $\pi$-Delocalization and bridge–perimeter destabilization lead to the fact that **1b** and **1a** have comparable energies.

A basic problem of previous studies was that they were based on quantum chemical methods of low accuracy. Depending on whether HF or MP2 is used, the preference for different valence tautomeric forms is found, which holds also for the XC functionals of DFT, as we have demonstrated in this work for the first time. This leads to rather limited insight into the possible cause of a quantum mechanical (electronic structure) effect. For example, Simonetta and co-workers[101] have used Hoffmann's approach[62,102] to rationalize the stability of substituted cyclopropanes to explain substituent effects in bridged [10]annulenes where their arguments were based on low level calculations. As was pointed out by Cremer and co-workers,[62] the orbital model used does not even explain all substituent effects for cyclopropanes. Furthermore, it does not consider the impact of bridge–perimeter interactions, the stabilization of biradicaloid structures for medium-sized $R$ values by conjugation, or the dynamic aspects of the valence tautomeric rearrangement.

Similarly, use of the topological analysis of $\rho(\mathbf{r})$ by Gatti and co-workers,[40] results of which were interpreted as proof for a long covalent C1C6 bond, have to be criticized because they were carried out at the HF/minimal basis set level without using any quantum mechanical criterion for covalent bonding. Other investigations were based on the NBO analysis or heuristic models utilizing the degree of bond length alternation in the ring perimeter.[42] These studies were insofar questionable as the properties analyzed were not referenced with regard to a suitable reference system.

An interesting rationalization of the carrying dynamic behavior of bridged [10]annulenes was proposed by Choi and Kertesz,[32] who model the opening of the cyclopropane ring


dx.doi.org/10.1021/jp5082966 | J. Phys. Chem. A 2015, 119, 1666–1682

in **1** or **2** by its conversion into a trimethylene biracial in its triplet ground state. The stabilization of the triplet trimethylene by substituents as described by DFT provides then a basis to understand whether the bisnorcaradiene or annulene form is more stabilized. We note in this connection that the radical centers are part of a conjugated system, and a more realistic model would be the opening of 3-substituted 1,2-divinylcyclopropanes.

Dorn and co-workers[50] excluded, on the basis of $^{13}$C CPMAS (cross-polarization magic angle spinning) spectra, a rapid valence−tautomeric process for **1**. Instead, these authors suggested that an asymmetric PEC and a different population of the vibrational levels at higher temperature would lead to the observed temperature dependence of the NMR spectra. Alternatively, temperature dependent intermolecular interactions could cause the observed temperature dependence.[50] Our high level quantum chemical results are in line with the first explanation whereas strong intermolecular interactions cannot be confirmed.

Kaupp and Boy[103] analyzed the measured temperature factors of the crystal data and concluded that a structural disorder in the solid state leads to the coexistence of bisnorcaradiene and [10]annulene, which would imply that the measured $R$ values are just averages. Our results do not agree with this hypothesis, as the modeling of packing effects using a tetramer of **1** leads to changes in $R$ that are in the range of $R$ differences measured by X-ray diffraction.[44]

## 5. CONCLUSIONS

This investigation provides a convincing explanation for the puzzling observations made in connection with molecule **1**. This explanation is based on extensive calculations with more than 20 different quantum chemical methods and the analysis of energy, geometry, dipole moment, charge transfer, NMR chemical shifts, indirect spin−spin coupling constants, local vibrational modes, and electron and energy density changes given as a function of the critical distance $R$(C1C6). Our work has led to a number of methodological insights and experimentally relevant conclusions, which are of general relevance for future experimental or theoretical work on related molecules, especially in connection with materials science.

(1) The investigation presented here reveals that system **1** possesses a broad, slightly asymmetric SW potential (or a very flat DW minimum) in which it carries out a large C1C6 amplitude vibration. Forms **1b** and **1a** have almost identical relative energies and enthalpies. A methodologically independent determination of the critical distance $R$ based on a comparison of measured and calculated $^{13}$C NMR chemical shifts leads to a value of 1.775 Å. By using only those shift values strongly dependent on $R$, the NMR-based determination of $R$ can be improved to 1.79 Å in line with the X-ray diffraction values of 1.780(7) and 1.836(7) Å.[44]

(2) This work suggests that the $R$ value in solution corresponds to a time-averaged value whereas the $R$ values of the unit cell are adopted by molecules of **1** being exposed to different packing effects. Our investigation could confirm the existence of packing effects using small models (dimer, tetramer.) For a tetramer model, a $\Delta R$ value of 0.023 Å was calculated suggesting a structure distortion as it was found in the solid state: $\Delta$R = 0.056 Å determined by the X-ray diffraction analysis.[44]

(3) The peculiar valence tautomeric potential of **1** is the result of the destabilization of the annulene form by introducing steric strain via the geminal dimethyl group. This is a direct consequence of balancing methyl-perimeter exchange repulsion against (electrostatic or dispersion driven) attraction. $\pi$-delocalization stabilizes the biradicaloid structure generated for medium-sized $R$ values, which otherwise would lead to a relatively high barrier of valence tautomerization. Without the methyl-annulene interactions, $\pi$-delocalization and the resulting aromatic 10$\pi$-stabilization would shift the global minimum always to **1a**.

(4) The analysis of the vibrational modes of **1** as well as its electron and energy density distribution reveals that covalent C1C6 bonding ceases to exist beyond R = 1.7 Å on to larger values of $R$. Hence, at 1.8 Å one can only speak of homoaromatic through-space interactions, which will play little role for distances larger than 2 Å, i.e. for the annulenic form.

(5) In the course of this work, it became necessary to accurately determine the PEC of the parent system **2**. CASPT2(14,14) calculations predict a SW potential with a shoulder between 1.6 and 1.9 Å. For an assumed $R$ value of 1.70 Å, the bis norcaradiene form has a relative enthalpy $\Delta H(298)$, which is 10.2 kcal/mol higher than that of the annulene form, i.e. at room temperature the percentage of bisnorcaradine is finite but close to zero.

(6) Because of its close relationship to systems **1** and **2**, we investigated also the valence-tautomeric system **3**. The CASPT2(10,10)-based free activation energy $\Delta G^a(298)$ of cycloheptatriene rearranging to norcaradiene is 12.2 kcal/mol in forward and 6.0 kcal/mol in the reverse reaction where the latter value is identical to a kinetic value obtained at 110 K, but 1.2 kcal/mol smaller than a derived value at 298 K obtained in the same study.[93] We show that the latter deviation is caused by an overly large entropy change $\Delta S^a$ used in the experimental study. The $\Delta G(298)$ value of **3b** relative to **3a** is 6.2 kcal/mol. The latter value replaces a previous NMR-based estimate of 4 ± 2 kcal/mol.[93,104] The concentration of **3b** at room temperature is just 0.003% rather than the previously estimated value of 0.1%.

(7) Although **1**, **2**, and **3** are closed shell molecules, their description requires the inclusion of both dynamical and nondynamical electron correlation to a high degree, i.e. for the former T excitations are absolutely necessary as is a (14,14) active space (because of $\sigma - \pi$ mixing and conjugative stabilization of a transient biradicaloid) provided at least second order perturbation theory is used. Ideally, these systems would be investigated with MR-AQCCSD based on a large active space. A basis set of VTZ quality is absolutely needed, because the calculations of this work reveal that an augmentation with diffuse functions is also required together with the multireference description and the T dynamical correlation effects. This is currently beyond computational possibilities but will be a target for future studies.

(8) This work has also shown the usefulness of long-range exact exchange and the promising performance of double-hybrid XC functionals. We suggest that the energetics for **1**, **2**, and **3** obtained in this work will be included in the standard reaction sets for the testing of new XC functionals. We see the possibility of combining different flavors of MP2 spin scaling and dispersion corrections in a double-hybrid functional to get more accurate results, as is obtained with the B2PLYPD functional in this work.

(9) The bridged annulenes synthesized in the Vogel group have so far evaded thorough quantum chemical investigations, as they can only be accurately described by combining


dx.doi.org/10.1021/jp5082966 | J. Phys. Chem. A 2015, 119, 1666−1682

dynamical and nondynamical electron correlation in a post-HF method. This work shows that the active space has to include also the $\sigma$ orbitals (or Walsh-orbitals) of the annulene bridge to describe $\pi$-delocalization reliably. A quantum chemical investigation of the bridged annulenes can predict those properties that may be interesting in connection with polymer chemistry, materials chemistry, or nanochemistry. We note in this connection that the synthesis of bridged annulenes involves carbene addition, which is a technique more and more used in fullerene chemistry where systems with perturbed $\pi$-delocalization and specific material properties are generated in this way. The procedures used in this work would also be useful for the quantum chemical investigation of these systems employing fine-tuned double hybrid functionals.

(10) Finally, it is noteworthy that a system such as **1** is the basis for a molecular switch, which by ring substitution or suitable interactions with the environment can be pushed into an on- (e.g., **1b**) or off-position (**1a**).

## ■ ASSOCIATED CONTENT

### Supporting Information

Discussion of the calculated PECs as they reveal advantages and disadvantages of a given method, and calculated geometries, energies, and other properties for all molecules summarized in 24 tables. This material is available free of charge via the Internet at http://pubs.acs.org.

## ■ AUTHOR INFORMATION

### Corresponding Author

*E-mail: dcremer@smu.edu.

### Notes

The authors declare no competing financial interest.

## ■ ACKNOWLEDGMENTS

This work was financially supported by the National Science Foundation, Grant CHE 1152357. We thank SMU for providing computational resources. An early investigation of **1** and **2** by Elfi Kraka is acknowledged. Thanks also to Marek Freindorf, Dani Setiawan, and Rob Kalescky for help with some of the calculations.

## ■ REFERENCES

(1) Pauling, L. C. *The Nature of the Chemical Bond and the Structure of Molecules and Crystals*, 3rd ed.; Cornell University Press: Ithaca, NY, 1960.

(2) Kalescky, R.; Kraka, E.; Cremer, D. Identification of the Strongest Bonds in Chemistry. *J. Phys. Chem. A* **2013**, *117*, 8981−8995.

(3) Schreiner, P. R.; Chernish, L. V.; Gunchenko, P. A.; Tikhonchuk, E. Y.; Hausmann, H.; Serafin, M.; Schlecht, S.; Dahl, J. E. P.; Carlson, R. M. K.; Fokin, A. A. Overcoming Lability of Extremely Long Alkane Carbon-Carbon Bonds Through Dispersion Forces. *Nature* **2011**, *477*, 308−311.

(4) Suzuki, T.; Uchimura, Y.; Ishigaki, Y.; Takeda, T.; Katoono, R.; Kawai, H.; Fujiwara, K.; Nagaki, A.; Yoshida, J. Nonadditive Substituent Effects on Expanding Prestrained C-C Bond in Crystal: X-ray Analyses on Unsymmetrically Substituted Tetraarylpyracenes Prepared by a Flow Microreactor Method. *Chem. Lett.* **2012**, *41*, 541−543.

(5) Grimme, S.; Schreiner, P. R. Steric Crowding Can Stabilize a Labile Molecule: Solving the Hexaphenylethane Riddle. *Angew. Chem., Int. Ed. Engl.* **2011**, *50*, 12639−12642.

(6) Kawai, H.; Takeda, T.; Fujiwara, K.; Wakeshima, M.; Hinatsu, Y.; Suzuki, T. Ultralong Carbon-Carbon Bonds in Dispirobis(10-methylacridan) Derivatives with an Acenaphthene, Pyracene, or Dihydropyracylene Skeleton. *Chem.—Eur. J.* **2008**, *14*, 5780−5793.

(7) Suzuki, T.; Takeda, T.; Kawai, H.; Fujiwara, K. Ultralong C-C Bonds in Hexaphenylethane Derivatives. *Pure Appl. Chem.* **2008**, *80*, 547−553.

(8) Tanaka, K.; Takamoto, N.; Tezuka, Y.; Kato, M.; Toda, F. Preparation and Structural Study of Naphtho- and Anthrocyclobutene Derivatives Which Have Extremely Long C-C Bonds. *Tetrahedron* **2001**, *57*, 3761−3767.

(9) Grafenstein, J.; Kraka, E.; D. Cremer, D. The Impact of the Self-interaction Error on the Density Functional Theory Description of Dissociating Radical Cations: Ionic and Covalent Dissociation Limits. *J. Chem. Phys.* **2004**, *120*, 524−539.

(10) Cremer, D.; Childs, R. F.; Kraka, E. In *The Chemistry of Functional Groups, The Chemistry of the Cyclopropyl Group*; Rappoport, Z., Ed.; Wiley: Chichester, UK, 1995; Vol. *2*, pp 339−410.

(11) Childs, R. F.; Cremer, D.; Elia, G. In *The Chemistry of Functional Groups, The Chemistry of the Cyclopropyl Group*; Rappoport, Z., Ed.; Wiley: Chichester, UK, 1995; Vol. *2*, pp 411−468.

(12) Oliva, J. M.; Allan, N. L.; Schleyer, P.; Vinas, C.; Teixidor, F. Strikingly Long C··· C Distances in 1,2-Disubstituted ortho-Carboranes and Their Dianions. *J. Am. Chem. Soc.* **2005**, *127*, 13538−13547.

(13) Wannere, C. S.; Chen, Z.; Schleyer, P. *Carbocation Chemistry—Zwitterionic "Neutral" and "Anionic" Carbocation Analogs*; Wiley: Hoboken, NJ, 2004.

(14) Huang, J.; Sumpter, B.; Meunier, V.; Tian, Y.; Kertesz, M. Cyclo-biphenalenyl Biradicaloid Molecular Materials: Conformation, Tautomerization, Magnetism, and Thermochromism. *Chem. Mater.* **2011**, *23*, 874−885.

(15) Jose, D.; Datta, A. Role of Multicentered Bonding in Controlling Magnetic Interactions in $\pi$ -Stacked Bis-Dithiazolyl Radical. *Cryst. Growth Des.* **2011**, *11*, 3137−3140.

(16) Mota, F.; Miller, J.; Novoa, J. J. Comparative Analysis of the Multicenter, Long Bond in $[TCNE]^-$ and Phenalenyl Radical Dimers: A Unified Description of Multicenter, Long Bonds. *J. Am. Chem. Soc.* **2009**, *131*, 7699−7707.

(17) Capdevila-Cortada, M.; Novoa, J. J. The Nature of the $[TTF]^{+}\cdots[TTF]^{+}$ Interactions in the $[TTF]_2^{2+}$ Dimers Embedded in Charged [3]Catenanes: Room-Temperature Multicenter Long Bonds. *Chem.—Eur. J.* **2012**, *18*, 5335−5344.

(18) Novoa, J. J.; Lafuente, P.; Del Sesto, R. E.; Miller, J. S. Exceptionally Long (>2.9 Å) C-C Bonds Between $[TCNE]^-$ Ions: Two-Electron, Four-Center $\pi^*$—$\pi^*$ C-C Bonding in $\pi$−$[TCNE]_2^{2-}$. *Angew. Chem., Int. Ed.* **2001**, *40*, 2540−2545.

(19) Garcia-Yoldi, I.; Miller, J.; Novoa, J. Theoretical Study of the Electronic Structure of $[TCNQ]_2^{2-}$ (TCNQ = 7,7,8,8-Tetracyano-p-quinodimethane) Dimers and Their Intradimer, Long, Multicenter Bond in Solution and the Solid State. *J. Phys. Chem. A* **2009**, *113*, 7124−7132.

(20) Novoa, J. J.; Stephens, P. W.; Weerasekare, M.; Shum, W. W.; Miller, J. S. The Tetracyanopyrazinide Dimer Dianion, $[TCNP]_2^{2-}$ Electron 8-Center Bonding. *J. Am. Chem. Soc.* **2009**, *131*, 9070−9075.

(21) Jackowski, J.; Simons, J. Theoretical Analysis of the Electronic Structure and Bonding Stability of the TCNE Dimer Dianion $(TCNE)_2^{2-}$. *J. Am. Chem. Soc.* **2003**, *125*, 16089−16096.

(22) Plitzko, K.; Rapko, B.; Gollas, B.; Wehrle, G.; Weakley, T.; Pierce, D. T.; Geiger, W. E.; Haddon, R. C.; Boekelheide, V. Bis($\eta^6$-hexamethylbenzene)($\eta^6$, $\eta^6$-[2n]cyclophane)diruthenium(II,II) Complexes and Their Two-Electron Reduction to [2n]Cyclophane Derivatives Having Two Cyclohexadienyl Anion Decks Joined by an Extremely Long Carbon-Carbon Bond. *J. Am. Chem. Soc.* **1990**, *112*, 6545−6556.

(23) Vogel, E.; Roth, H. D. The Cyclodecapentaene System. *Angew. Chem., Int. Ed. Engl.* **1964**, *3*, 228−229.

(24) Dobler, M.; Dunitz, J. Die Kristallstruktur der 1,6-Methano-cyclodecapentaen-2-carbonsaure. *Helv. Chim. Acta* **1965**, *48*, 1429−1440.

(25) Bianchi, R.; Pilati, T.; Simonetta, M. Structure of 1,6-Methano[10]Annulene. *Acta Crystallogr., Sect. B: Struct. Crystallogr. Cryst. Chem.* **1980**, *B36*, 3146−3148.
(26) Blattmann, H.; Boll, W.; Heilbronner, E.; Hohlneicher, G.; Vogel, E.; Weber, J. Die Elektronenzustande von Perimeter-π-Systemen: I. Die Elektronenspektren 1,6-überbriickter [10]-Annulene. *Helv. Chim. Acta* **1966**, *49*, 2017−2038.
(27) Gramaccioli, C. M.; Simonetta, M. The Structure of 11,11-Difluoro-1,6-methano[l0]annulene. *Acta Crystallogr.* **1965**, *B27*, 2231−2237.
(28) Günther, H.; Shyoukh, A.; Cremer, D.; Frisch, K. H. Q-method Electronic Ground State Properties of Annulenes: Experimental Test of the Q-Value Method. *Tetrahedron Lett.* **1974**, *9*, 781−783.
(29) Birgi, H.; Schefter, E.; Dunitz, J. Chemical Reaction Paths—VI: A Pericyclic Ring Closure. *Tetrahedron* **1975**, *31*, 3089−3092.
(30) Dewey, H.; Deger, H.; Frolich, W.; Dick, B.; Klingensmith, K.; Hohlneicher, G.; Vogel, E.; Michl, J. Excited States of Methano-Bridged [10]-, [14]-, and [18]Annulenes. Evidence for Strong Transannular Interaction, and Relation to Homoaromaticity. *J. Am. Chem. Soc.* **1980**, *102*, 6412−6417.
(31) Klingensmith, K.; Puttmann, W.; Vogel, E.; Michl, J. Applications of MCD Spectroscopy: MO Ordering and Transannular Interaction in 1,6-Methano[10]annulenes from Analysis of Substituent Effects. *J. Am. Chem. Soc.* **1983**, *105*, 3375−3380.
(32) Choi, C. H.; Kertesz, M. New Interpretation of the Valence Tautomerism of 1,6-Methano[10]annulenes and Its Application to Fullerene Derivatives. *J. Phys. Chem. A* **1998**, *102*, 3429−3437.
(33) Catani, L.; Gellini, C.; Salvi, P. Excited States of 1,6-Methano[10]annulene: Site Selection Fluorescence and Fluorescence Excitation Spectroscopy on S1. *J. Phys. Chem. A* **1998**, *102*, 1945−1953.
(34) Gellini, C.; Salvi, P.; Vogel, E. Ground State of 1,6-Bridged [10] Annulenes: Infrared and Raman Spectra and Density Functional Calculations. *J. Phys. Chem. A* **2000**, *104*, 3110−3116.
(35) Vogel, E. Aromatic 10- and 14-π-Electron Systems. *Proc. R. A. Welch Found. Conf. Chem. Res.* **1969**, *12*, 215−251.
(36) Balaban, A. T.; Banciu, M.; Ciorba, V. *Annulenes, Benzo-, Hetero-, Homo-Derivatives and their Valence Isomers*; CRC Press: Boca Raton, FL, 1987.
(37) Kuroda, S.; Kajioka, T.; Fukuta, A.; Thanh, N. C.; Zhang, Y.; Miyatake, R.; Mouri, M.; Zuo, S.; Oda, M. Revisitation of Cycloheptatriene Derivatives as a Building Block for Various Substituted and Fused 1,6-Methano[10]annulenes and Substituted 4,9-Methanothia[11]annulenes. *Mini-Rev. Org. Chem.* **2007**, *4*, 31−49.
(38) Cremer, D.; Dick, B. Theoretical Investigations on the Valence Tautomerism Between 1,6-Methano[10]annulene and [4.4.$1^{1,6}$]-Undeca-2,4,7,9-tetraene. *Angew. Chem.* **1982**, *94*, 865−866.
(39) Sironi, M.; Raimondi, M.; Cooper, D. L.; Gerratt, J. The Unusual Coordination of Carbon Atoms in Bicyclic 1,6-Methano[10]-annulene: A Modern Valence Bond Study. *J. Mol. Struct.: THEOCHEM* **1995**, *338*, 257−265.
(40) Gatti, C.; Barzaghi, M.; Simonetta, M. Charge Density Topological Approach to the Dinorcaradiene ⇄ [10]Annulene Equilibrium in Some 11,11-Disubstituted 1,6-Methano[10]annulenes. *J. Am. Chem. Soc.* **1985**, *107*, 878−887.
(41) Jiao, H.; Van Eikema Hommes, N. J. R.; Schleyer, P. Can Bridged 1,6-X-[10]Annulenes (X = SiH2, SiMe2, PH, and S) Exist? *Org. Lett.* **2002**, *4*, 2393−2396.
(42) Caramori, G. F.; de Oliveira, K. T.; Galembeck, S. E.; Bultinck, P.; Constantino, M. G. Aromaticity and Homoaromaticity in Methano[10]annulenes. *J. Org. Chem.* **2007**, *72*, 76−85.
(43) Gellini, C.; Salvi, P. R. Structures of Annulenes and Model Annulene Systems in the Ground and Lowest Excited States. *Symmetry* **2010**, *2*, 1846−1924.
(44) Bianchi, R.; Morosi, G.; Mugnoli, A.; Simonetta, M. The Influence of Substituents on the Equilbrium Bisnorcaradiene ⇄ [10]Annulene. The Crystal and Molecular Structure of 11,11-Dimethyltricyclo[4,4,1,$0^{1,6}$]undeca-2,4,7,9-tetraene. *Acta Crystallogr.* **1973**, *B29*, 1196−1208.
(45) Bianchi, R.; Pilati, T.; Simonetta, M. The Influence of Substituents on the Equilbrium Bisnorcaradiene ⇄ [10]Annulene. The Crystal and Molecular Structure of 11-Methyltricyclo[4,4,1,$0^{1,6}$]-undeca-2,4,7,9-tetraene-11-carbonitrile. *Acta Crystallogr.* **1978**, *B34*, 2157−2162.
(46) Vogel, E.; Scholl, T.; Lex, J.; Hohlneicher, G. Norcaradiene Valence Tautomer of a 1,6-Methano[10]Annulene: Tricyclo [4.4.1.$0^{1,6}$]undeca-2,4,7,9-tetraene-11,11-dicarbonitrile. *Angew. Chem., Int. Ed. Engl.* **1982**, *94*, 924−925.
(47) Günther, H.; Schmickler, H.; Bremser, W.; Straube, F. A.; Vogel, E. Application of Carbon-13 Resonance Spectroscopy. 6. Aromatic-olefin Equilibrium 1,6-Methano[10]annulenetricyclo[4.4.1.$0^{1,6}$]-undeca-2,4,7,9-tetraene Valence Tautomerism. *Angew. Chem., Int. Ed. Engl.* **1973**, *12*, 570−571.
(48) Arnz, R.; Carneiro, J. W.; Klug, W.; Schmickler, H.; Vogel, E.; Breuckmann, R.; Klarner, F. G. σ-Homoacenaphthylenes and π-Homoacenaphthenes. *Angew. Chem., Int. Ed. Engl.* **1991**, *30*, 683−686.
(49) Frydman, L.; Frydman, B.; Kustanovich, I.; Vega, S.; Vogel, E.; Yannoni, C. S. A Carbon-13 NMR Study of the Arene-Olefin Valence Tautomerism of 1,6-Methano[10]annulenes in the Solid Phase. *J. Am. Chem. Soc.* **1990**, *112*, 6472−6476.
(50) Dorn, H. C.; Yannoni, C. S.; Limbach, H.-H.; Vogel, E. Evidence for a Nonclassical Structure of a 1,6-Methano[10]annulene: A Cryogenic $^{13}$C CPMAS NMR Study of the 11,11-Dimethyl Derivative. *J. Phys. Chem.* **1994**, *98*, 11628−11629.
(51) Cremer, D. In *Encyclopedia of Computational Chemistry*; Schleyer, P. v. R., Allinger, N. L., Clark, T., Gasteiger, J., Kollman, P. A., Schaefer, H. F., Schreiner, P. R., Eds.; Wiley: Chichester, UK, 1998; Vol. 3, pp 1706−1735.
(52) Cremer, D. Møller-Plesset Perturbation Theory, From Small Molecule Methods to Methods for Thousands of Atoms. *Wiley Interdiscip. Rev.: Comput. Mol. Sci.* **2011**, *1*, 509−530.
(53) Becke, A. D. Density-Functional Thermochemistry. III. The Role of Exact Exchange. *J. Chem. Phys.* **1993**, *98*, 5648−5652.
(54) Stevens, P. J.; Devlin, F. J.; Chablowski, C. F.; Frisch, M. J. Ab Initio Calculation of Vibrational Absorption and Circular Dichroism Spectra Using Density Functional Force Fields. *J. Phys. Chem.* **1994**, *98*, 11623−11627.
(55) Purvis, I.; G. D; Bartlett, R. J. A Full Coupled-Cluster Singles and Doubles Model: The Inclusion of Disconnected Triples. *J. Chem. Phys.* **1982**, *76*, 1910−1918.
(56) Handy, N. C.; Pople, J. A.; Head-Gordon, M.; Raghavachari, K.; Trucks, G. W. Size-Consistent Brueckner Theory Limited to Double Substitutions. *Chem. Phys. Lett.* **1989**, *164*, 185−192.
(57) Raghavachari, K.; Trucks, G. W.; Pople, J. A.; Head-Gordon, M. A Fifth-Order Perturbation Comparison of Electron Correlation Theories. *Chem. Phys. Lett.* **1989**, *157*, 479−483.
(58) Raghavachari, K.; Pople, J. A.; Replogle, E. S.; Head-Gordon, M.; Handy, N. C. Size-consistent Brueckner Theory Limited to Double and Triple Substitutions. *Chem. Phys. Lett.* **1990**, *167*, 115−121.
(59) Malmqvist, P. A.; Roos, B. O. The CAS-SCF State Interaction Method. *Chem. Phys. Lett.* **1989**, *155*, 189−194.
(60) Andersson, K.; Malmqvist, P. A.; Roos, B. O.; Sadlej, A. J.; Wolinski, K. Second-Order Perturbation Theory with a CASSCF Reference Function. *J. Phys. Chem.* **1990**, *94*, 5483−5488.
(61) Havenith, R. W. A.; Taylor, P. R.; Angeli, C.; Cimiraglia, R.; Ruud, K. Calibration of the n-Electron Valence State Perturbation Theory Approach. *J. Chem. Phys.* **2004**, *120*, 4619−4625.
(62) Cremer, D.; Kraka, E.; Szabo, K. J. In *The Chemistry of Functional Groups, The Chemistry of the Cyclopropyl Group*; Rappoport, Z., Ed.; Wiley: Chichester, UK, 1995; Vol. 2, pp 43−137.
(63) Szalay, R. J.; Bartlett, R. J. Multireference Averaged Quadratic Coupled-Cluster Method: A Size-Extensive Modification of Multi-Reference CI. *Chem. Phys. Lett.* **1993**, *214*, 481−488.
(64) Stanton, J. F.; Gauss, J. Analytic Energy Gradients for the Equation-of-Motion Coupled-Cluster Method: Implementation and Application to the HCN/HNC System. *J. Chem. Phys.* **1994**, *10*, 4695−4698.

(65) Mennucci, B.; Tomasi, J. Continuum Solvation Models: A New Approach to the Problem of Solute's Charge Distribution and Cavity Boundaries. *J. Chem. Phys.* **1994**, *106*, 5151−5158.
(66) Haynes, W. M.; Lide, D. R.; Bruno, T. J. *CRC Handbook of Chemistry and Physics*; CRC Press: Boca Raton, FL, 2013.
(67) Krishnan, R.; Binkley, J. S.; Seeger, R.; Pople, J. A. Self-Consistent Molecular Orbital Methods. *XX*. A Basis Set for Correlated Wave Functions. *J. Chem. Phys.* **1980**, *72*, 650−654.
(68) Weinhold, F.; Landis, C. R. *Valency and Bonding: A Natural Bond Orbital Donor-Acceptor Perspective*; Cambridge University Press: Cambrige, UK, 2003.
(69) Bader, R. F. W. *Atoms in Molecules—A Quantum Theory*; Oxford University Press: Oxford, UK, 1990.
(70) Cremer, D.; Kraka, E. A Description of the Chemical Bond in Terms of Local Properties of Electron Density and Energy. *Croat. Chem.* **1984**, *57*, 1259−1281.
(71) Cremer, D.; Kraka, E. Chemical Bonds Without Bonding Electron Density—Does the Difference Electron Density Analysis Suffice for a Description of the Chemical Bond? *Angew. Chem., Int. Ed. Engl.* **1984**, *23*, 627−628.
(72) Wolinski, K.; Hinton, J. F.; Pulay, P. Efficient Implementation of the Gauge-Independent Atomic Orbital Method for NMR Chemical Shift Calculations. *J. Am. Chem. Soc.* **1990**, *112*, 8251−8260.
(73) Olsson, L.; Cremer, D. Sum-Over-States Density Functional Perturbation Theory: Prediction of Reliable 13C, 15N, and 17O Nuclear Magnetic Resonance Chemical Shifts. *J. Chem. Phys.* **1996**, *105*, 8995−4006.
(74) Cremer, D.; Reichel, F.; Kraka, E. Homotropenylium Cation: Structure, Stability and Magnetic Properties. *J. Am. Chem. Soc.* **1991**, *113*, 9459−9466.
(75) Ottosson, C.-H.; Kraka, E.; Cremer, D. *Theory as a Viable Partner of Experiment—The Quest for Trivalent Silylium Ions in Solution*; Elsevier: Amsterdam, 1999; Vol. 6, pp 231−301.
(76) Sychrovsky, V.; Gräfenstein, J.; Cremer, D. Nuclear Magnetic Resonance Spin-Spin Coupling Constants from Coupled Perturbed Density Functional Theory. *J. Chem. Phys.* **2000**, *113*, 3530−3547.
(77) Konkoli, Z.; Cremer, D. A New Way of Analyzing Vibrational Spectra I. Derivation of Adiabatic Internal Modes. *Int. J. Quantum Chem.* **1998**, *67*, 1−9.
(78) Konkoli, Z.; Cremer, D. A New Way of Analyzing Vibrational Spectra III. Characterization of Normal Vibrational Modes in Terms of Internal Vibrational Modes. *Int. J. Quantum Chem.* **1998**, *67*, 29−41.
(79) Kraka, E.; Larsson, J.; Cremer, D. In *Theoretical Organic Chemistry (Theoretical and Computational Chemistry)*; Parkanyi, C., Ed.; Elsevier: Amsterdam, 1998; Vol. *5*, p 259.
(80) Zou, W.; Kalescky, R.; Kraka, E.; Cremer, D. Relating Normal Vibrational Modes to Local Vibrational Modes with the help of an Adiabatic Connection Scheme. *J. Chem. Phys.* **2012**, *137*, 084114.
(81) Zou, W.; Kalescky, E.; Kraka, E.; Cremer, D. Relating Normal Vibrational Modes to Local Vibrational Modes: Benzene and Naphthalene. *J. Mol. Model.* **2012**, *19*, 2865−2877.
(82) Zou, W.; Cremer, D. Properties of Local Vibrational Modes: The Infrared Intensity. *Theor. Chem. Acc.* **2014**, *133*, 1451−1−15.
(83) Freindorf, M.; Kraka, E.; Cremer, D. A Comprehensive Analysis of Hydrogen Bond Interactions Based on Local Vibrational Modes. *Int. J. Quantum Chem.* **2012**, *112*, 3174−3187.
(84) Kalescky, R.; Zou, W.; Kraka, E.; Cremer, D. Quantitative Assessment of the Multiplicity of Carbon-Halogen Bonds: Carbenium and Halonium Ions with F, Cl, Br, I. *J. Phys. Chem. A* **2014**, *118*, 1948−1963.
(85) Kraka, E.; Cremer, D. Characterization of CF Bonds with Multiple-Bond Character: Bond Lengths, Stretching Force Constants, and Bond Dissociation Energies. *ChemPhysChem* **2009**, *10*, 686−698.
(86) Kalescky, R.; Kraka, E.; Cremer, D. Description of Aromaticity with the Help of Vibrational Spectroscopy: Anthracene and Phenanthrene. *J. Phys. Chem. A* **2014**, *118*, 223−237.
(87) Werner, H. J.; Knowles, P. J.; Knizia, G.; Manby, F. R.; Schütz, M.; Celani, P.; Korona, T.; Lindh, R.; Mitrushenkov, A.; Rauhut, G.; et al. *MOLPRO*, Version 2010. 1. A Package of Ab Initio Programs; 2010; see http://www.molpro.net.
(88) Kraka, E.; Zou, W.; Filatov, M.; Grafenstein, J.; Izotov, D.; Gauss, J.; He, Y.; Wu, A.; Konkoli, Z.; Cremer, D.; et al. *COLOGNE2014*; 2014; see http://www.smu.edu/catco.
(89) Stanton, J. F.; Gauss, J.; Harding, M. E.; Szalay, P. G.; et al. *CFOUR*, A Quantum Chemical Program Package; 2010; see http://www.cfour.de.
(90) Frisch, M. J.; Trucks, G. W.; Schlegel, H. B.; Scuseria, G. E.; Robb, M. A.; Cheeseman, J. R.; Scalmani, G.; Barone, V.; Mennucci, B.; Petersson, G. A.; et al. *Gaussian 09*, Revision A.1; 2010; Gaussian Inc.: Wallingford, CT.
(91) Gorlitz, M.; Günther, H. Protonenresonanz-Spektroskopie Ungesattigter Ringsysteme-XIII. *Tetrahedron* **1969**, *25*, 4467−4480.
(92) Balci, M.; Fischer, H.; Ginther, H. The Dynamic Behavior of 2,4,6-Cycloheptatriene-1-carbaldehyde. *Angew. Chem.* **1980**, *92*, 316−317.
(93) Rubin, M. B. Photolysis of Two Tricyclic Nonenediones. Direct Observation of Norcaradiene. *J. Am. Chem. Soc.* **1981**, *103*, 7791−7792.
(94) Celik, M.; Balci, M. The Substituent Effect on the Cycloheptatriene-Norcaradiene Equilibrium. Reaction of Singlet Oxygen with Substituted Cycloheptatrienes. *ARKIVOC* **2007**, *8*, 150−162.
(95) Jarzecki, A. A.; Gajewski, J.; Davidson, E. R. Thermal Rearrangements of Norcaradiene. *J. Am. Chem. Soc.* **1999**, *121*, 6928−6935.
(96) Cremer, D.; Dick, B.; Christeu, D. Theoretical Determination of Molecular Structure and Conformation. 12. Puckering of 1,3,5-Cycloheptatriene, 1H-Azepine, Oxepine, and Their Norcaradienic Valence Tautomers. *J. Mol. Struct.: THEOCHEM* **1984**, *110*, 227−291.
(97) Scott, A. P.; Radom, L. Harmonic Vibrational Frequencies: An Evaluation of Hartree-Fock, Møller-Plesset, Quadratic Configuration Interaction, Density Functional Theory, and Semiempirical Scale Factors. *J. Phys. Chem.* **1996**, *100*, 16502−16513.
(98) Kalinowski, H.; Berger, S.; Braun, S. *$^{13}$C NMR Spectroscopy*, 1st ed.; Wiley: New York, 1991.
(99) Kraka, E.; Cremer, D. *Chemical Implications of Local Features of the Electron Density Distribution*; Springer Verlag: Heidelburg, 1990; Vol. 2; pp 457−542.
(100) Kraka, E.; Larsson, J.; Cremer, D. In *Vibrational Modes in Computational IR Spectroscopy*; Grunenberg, J., Ed.; Wiley: New York, 2010; pp 105−149.
(101) Simonetta, M.; Barzaghi, M.; Gatti, C. Cyclopropane Ring Closure in 11,11-Disubstituted 1,6-Methano[10]annulenes. *J. Mol. Struct.: THEOCHEM* **1986**, *138*, 39−50.
(102) Hoffmann, R. The Norcardiene-Cycloheptatriene Equilibrium. *Tetrahedron Lett.* **1970**, *33*, 2907−2909.
(103) Kaupp, G.; Boy, J. Overlong C-C Single Bonds. *Angew. Chem., Int. Ed. Engl.* **1997**, *36*, 48−49.
(104) Wehner, R.; Günther, H. Applications of Carbon-13 NMR Spectroscopy. XVII. The Carbon-13 NMR Spectrum of 1,3,5-Cycloheptatriene. *Chem. Ber.* **1974**, *107*, 3152−3153.